27

ORNL-2719
Chemistry-General
TID-4500 (14th ed.)

PHASE EQUILIBRIA IN THE SYSTEMS UF_4-ThF_4 AND LiF-UF_4-ThF_4

C. F. Weaver
R. E. Thoma
H. Insley
H. A. Friedman

OAK RIDGE NATIONAL LABORATORY
operated by
UNION CARBIDE CORPORATION
for the
U.S. ATOMIC ENERGY COMMISSION

CONTENTS

ORNL-2719
Chemistry-General
TID-4500 (14th ed.)

Contract No. W-7405-eng-26

REACTOR CHEMISTRY DIVISION

PHASE EQUILIBRIA IN THE SYSTEMS UF_4–ThF_4 AND LiF-UF_4-ThF_4

C. F. Weaver
R. E. Thoma
H. Insley
H. A. Friedman

DATE ISSUED

AUG 17 1959

OAK RIDGE NATIONAL LABORATORY
Oak Ridge, Tennessee
operated by
UNION CARBIDE CORPORATION
for the
U.S. ATOMIC ENERGY COMMISSION

PHASE EQUILIBRIA IN THE SYSTEMS UF_4-ThF_4 AND LiF-UF_4-ThF_4

C. F. Weaver R. E. Thoma H. Insley H. A. Friedman

SUMMARY

As part of a study of materials potentially useful as fluid fuels for high-temperature reactors, equilibrium diagrams for the condensed systems UF_4-ThF_4 and LiF-UF_4-ThF_4 have been determined. Both thermal analysis and quenching techniques were used, with phase identification accomplished by petrographic and x-ray diffraction analysis. A complete series of solid solutions without maximum or minimum is formed by UF_4 and ThF_4. The system LiF-UF_4-ThF_4 contains no ternary compounds but does contain four ternary solid solutions. The compounds LiF·4ThF_4 and LiF·4UF_4 form a continuous series of solid solutions, as do the compounds 7LiF·6ThF_4 and 7LiF·6UF_4. A series of solid solutions exists having compositions at 33⅓ mole % LiF between LiF·2ThF_4 and 23 mole % UF_4. Another series of solid solutions exists having compositions at 75 mole % LiF between 3LiF·ThF_4 and 15.5 mole % UF_4. Seven primary-phase fields appear in the system, those which are solid solutions being indicated by (ss): LiF, 4LiF·UF_4, 3LiF·Th(U)F_4 (ss), 7LiF·6ThF_4–7LiF·6UF_4 (ss), LiF·2Th(U)F_4 (ss), LiF·4ThF_4–LiF·4UF_4 (ss), and UF_4-ThF_4 (ss). Phase relations were established from the liquidus to about 300°C. The three invariant points which occur are the following: peritectic, 19 mole % UF_4, 18 mole % ThF_4, 609°C; peritectic, 20.5 mole % UF_4, 7 mole % ThF_4, 500°C; and eutectic, 26.5 mole % UF_4, 1.5 mole % ThF_4, 488°C.

The solid phases taking part in the invariant reactions are the following: peritectic point at 609°C: LiF·4ThF_4–LiF·4UF_4 (ss) containing 28 mole % UF_4, LiF·2Th(U)F_4 containing 23 mole % UF_4, and 7LiF·6ThF_4–7LiF·6UF_4 containing 23 mole % UF_4; peritectic point at 500°C: LiF, 7LiF·6ThF_4–7LiF·6UF_4 (ss) containing 31 mole % UF_4, and 3LiF·Th(U)F_4 (ss) containing 15.5 mole % UF_4; eutectic point at 488°C: 4LiF·UF_4, LiF, and 7LiF·6ThF_4–7LiF·6UF_4 (ss) containing 42.5 mole % UF_4.

The refractive indices of the ternary solid solutions were determined as functions of composition and used for an optical analysis of the solid solutions when they occurred with other phases. This information made possible the construction of tie lines, fractionation paths, and compatibility triangles for the three ternary invariant points.

INTRODUCTION

Several years ago, R. C. Briant of the Oak Ridge National Laboratory suggested the use of a molten mixture of UF_4 and ThF_4 together with fluorides of alkali metals and beryllium fluoride or zirconium fluoride as a potential fuel for a high-temperature, low-pressure nuclear reactor.[1] A systematic study at ORNL during the past several years has developed molten salt mixtures whose chemical and physical properties seem to suit them for use as fuels in U^{235} burner reactors,[2] in plutonium burner reactors, and in one-region U^{233} breeder reactors and as blankets in two-region U^{233} breeder reactors. Nuclear reactor designs have been proposed which would utilize mixtures of Li^7F, BeF_2, ThF_4, and UF_4 as fuels.[3–5]

Little is known concerning the phase relationships of the system LiF-BeF_2-UF_4-ThF_4 except that solid solutions involving LiF, UF_4, and ThF_4 occur as primary and secondary phases at low UF_4 and ThF_4 concentrations. Phase diagrams of the limiting binary systems LiF-BeF_2 (ref 6), LiF-UF_4 (ref 7), and LiF-ThF_4 (ref 8)

---

[1] A. M. Weinberg and R. C. Briant, *Nuclear Sci. and Eng.* 2, 797–803 (1957).

[2] E. S. Bettis *et al.*, *Nuclear Sci. and Eng.* 2, 804–825 (1957).

[3] J. K. Davidson and W. L. Robb, *A Molten Salt Thorium Converter for Power Production*, KAPL-M-JKD-10 (1956).

[4] L. G. Alexander *et al.*, "Conceptual Design of a Power Reactor," chap 17 of *Fluid Fuel Reactors*, Addison-Wesley, Reading, Mass., 1958.

[5] L. G. Alexander, "Nuclear Aspects of Molten-Salt Reactors," chap 14 of *Fluid Fuel Reactors*, Addison-Wesley, Reading, Mass., 1958.

[6] R. E. Thoma, *Phase Diagrams of Nuclear Reactor Materials*, ORNL-2548.

[7] C. J. Barton *et al.*, *J. Am. Ceram. Soc.* 41(2), 63–69 (1958).

[8] R. E. Thoma *et al.*, "Phase Equilibria in the Fused Salt Systems LiF-ThF_4 and NaF-ThF_4," *J. Phys. Chem.* (in press).

have been published. The systems BeF_2-UF_4 (ref 9) and LiF-BeF_2-UF_4 (ref 10) have been investigated at the Mound Laboratory. Results of phase equilibrium studies of the systems BeF_2-ThF_4 and LiF-BeF_2-ThF_4 will soon be reported by the authors. Preliminary diagrams of these systems are in the literature.[11,12] The system BeF_2-UF_4-ThF_4 has not, to our knowledge, been investigated. The remaining systems, UF_4-ThF_4 and LiF-UF_4-ThF_4, are the subject of this report. Preliminary diagrams of these systems have been reported by the authors.[12,13] As is to be expected from the known similarities in the parameters of the unit cells of ThF_4 and UF_4 (refs 14 and 15), a salient characteristic of the condensed systems UF_4-ThF_4 and LiF-UF_4-ThF_4 is the extensive formation of solid solutions.

MATERIALS, METHODS, AND APPARATUS

The lithium fluoride used in this investigation was reagent grade, obtained from Foote Mineral Company and from Maywood Chemical Works. The thorium tetrafluoride was obtained from Iowa State College and from National Lead Company. The uranium tetrafluoride was obtained from Mallinkrodt Chemical Works. No appreciable impurities were found in the uranium tetrafluoride or thorium tetrafluoride by spectrographic, x-ray diffraction, or microscopic analysis.

The phase equilibria data were obtained by thermal analysis of slowly cooled melts and by identifying the phases present in mixtures which had been equilibrated and quenched. Because uranium and thorium fluorides are easily converted to oxides or oxyfluorides at elevated temperatures, it was necessary to remove small amounts of water and oxygen as completely as possible from the starting materials. To facilitate the removal of these substances, ammonium bifluoride was added to the mixtures of lithium fluoride, thorium fluoride, and uranium fluoride before initial heating in the thermal analysis experiments. While the mixtures were being heated the water was evaporated from the system. The oxides were converted by reaction with the ammonium bifluoride to products which have not yet been identified but which are likely to be ammonium fluometallates.[16,17] Upon further heating, the "ammonium fluometallates" decomposed to form the metal fluorides. These same mixtures were later used in the quenching experiments.

The phases were identified by petrographic and x-ray diffraction techniques. These methods for characterizing phases, as well as a description of the apparatus used for preparing and annealing samples, were reported previously.[7,8,18–21]

GENERAL DISCUSSION OF THE SYSTEM LiF-UF_4-ThF_4 AND THE LIMITING BINARY SYSTEMS

The phase diagram of the condensed ternary system LiF-UF_4-ThF_4 is shown in Fig. 1, and a photograph of a three-dimensional model[22] of the system is shown in Fig. 2. The associated binary systems are shown in Figs. 3–5.

One metastable compound (3LiF·UF_4) and three incongruently melting compounds (4LiF·UF_4, 7LiF·6UF_4, and LiF·4UF_4) are formed in the system LiF-UF_4. Optical properties, except those of 3LiF·UF_4, and x-ray diffraction data for these

---

[9] J. F. Eichelberger, E. F. Joy, E. Orban, T. B. Rhinehammer, and P. A. Tucker, unpublished work.

[10] J. F. Eichelberger, D. E. Etter, C. R. Hudgens, L. V. Jones, T. B. Rhinehammer, P. A. Tucker, and L. J. Wittenberg, unpublished work.

[11] W. R. Grimes *et al.*, "Chemical Aspects of Molten-Fluoride Reactor Fuels," chap 12 of *Fluid Fuel Reactors*, Addison-Wesley, Reading, Mass., 1958.

[12] "Supplement to 'Phase Diagrams for Ceramists'" (compiled by E. M. Levin and H. F. McMurdie), American Ceramics Society, Inc., Easton, Pa. (in press).

[13] R. E. Thoma *et al.*, *MSR Quar. Prog. Rep. Jan 31, 1958*, ORNL-2474, p 81.

[14] W. H. Zachariasen, *X-Ray Diffraction Studies of Miscellaneous Uranium Compounds*, MDDC-1152 (June 1946).

[15] J. J. Katz and E. Rabinowitch, *The Chemistry of Uranium*, NNES VIII-5, McGraw-Hill, New York, 1951.

[16] *MSR Quar. Prog. Rep. April 30, 1959*, ORNL-2723, p 93.

[17] B. J. Sturm, Oak Ridge National Laboratory, personal communication.

[18] C. J. Barton *et al.*, *J. Phys. Chem.* 62, 665 (1958).

[19] R. E. Thoma *et al.*, *J. Am. Ceram. Soc.* 42(1), 21–26 (1959).

[20] H. A. Friedman, "Modifications of Quenching Techniques for Phase Equilibrium Studies," *J. Am. Ceram. Soc.* (in press).

[21] P. A. Tucker and E. F. Joy, *Am. Ceram. Soc. Bull.* 36(2), 52–54 (1957).

[22] Model constructed by C. Johnson, summer participant at ORNL, 1958.

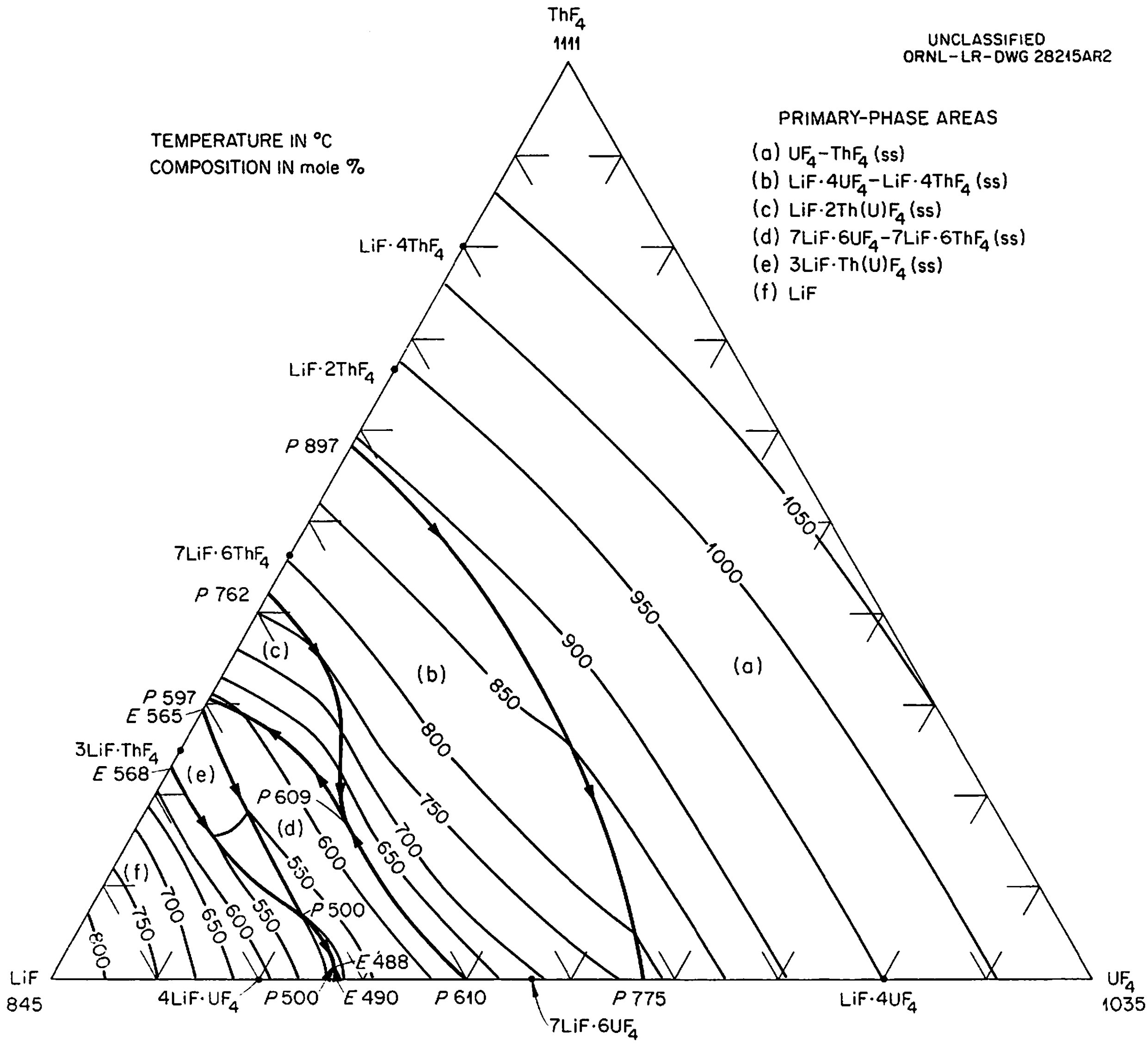

Fig. 1. The System LiF-UF_4-ThF_4.

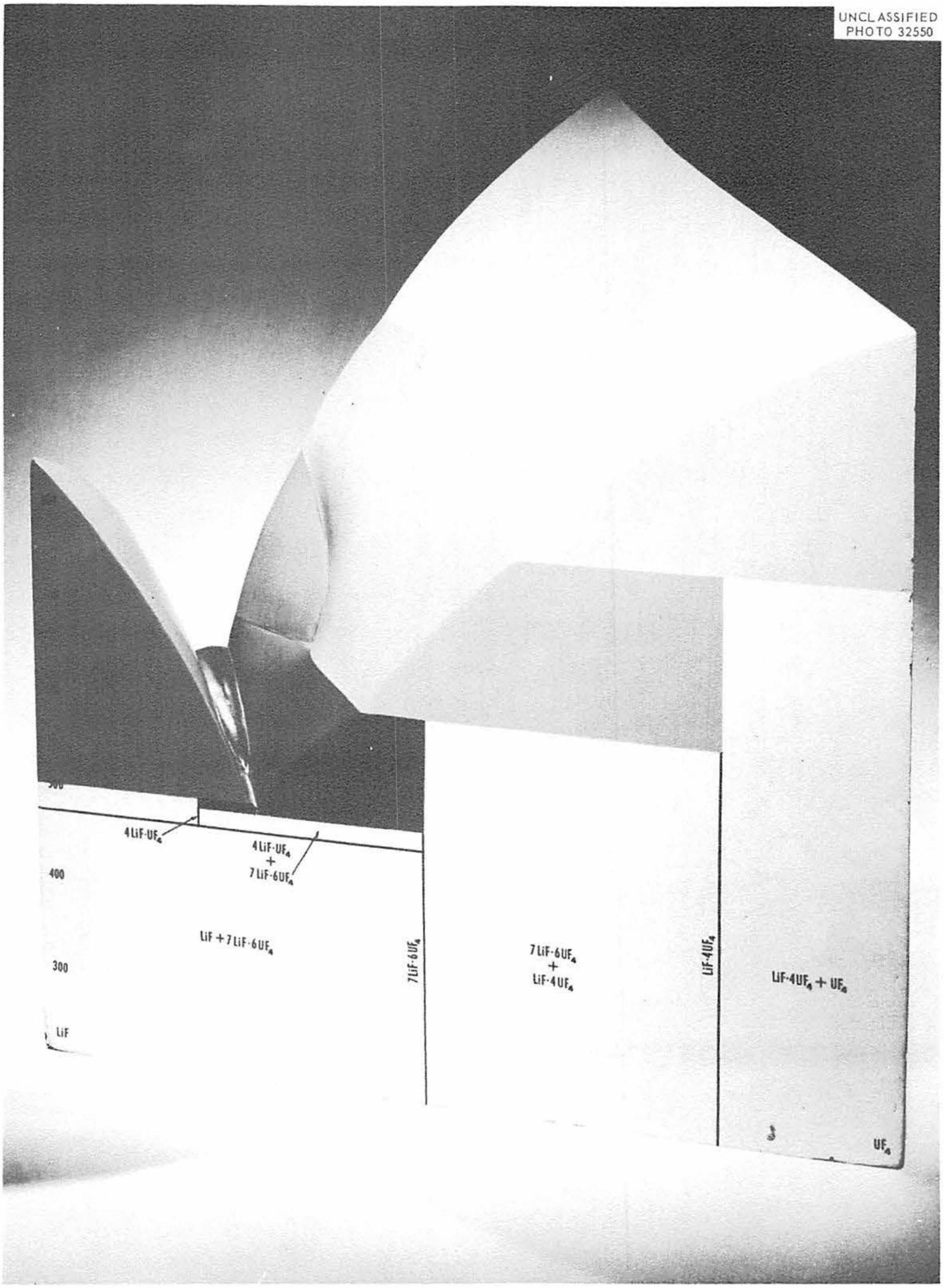

Fig. 2. Three-Dimensional Model of the System $LiF-UF_4-ThF_4$.

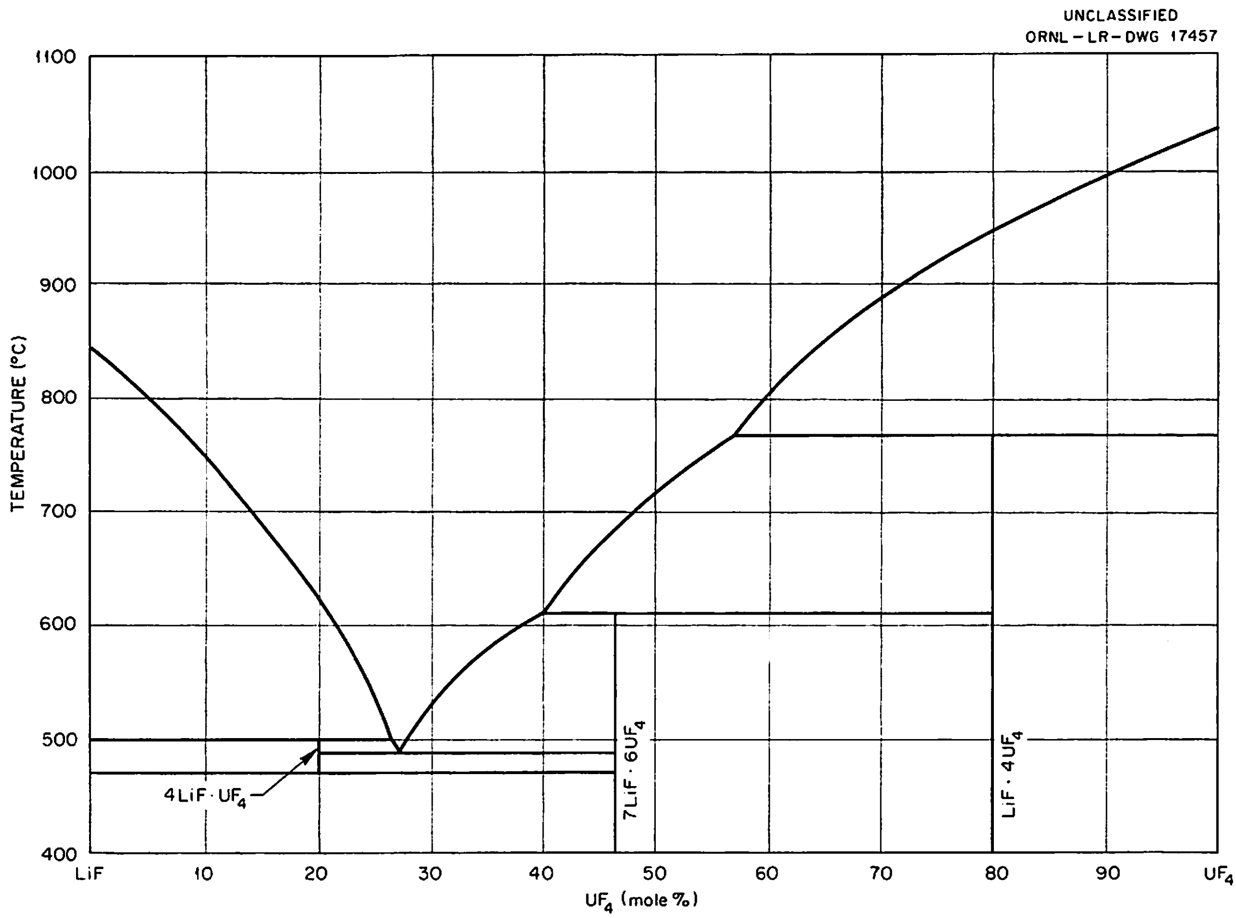

Fig. 3. The System $LiF-UF_4$.

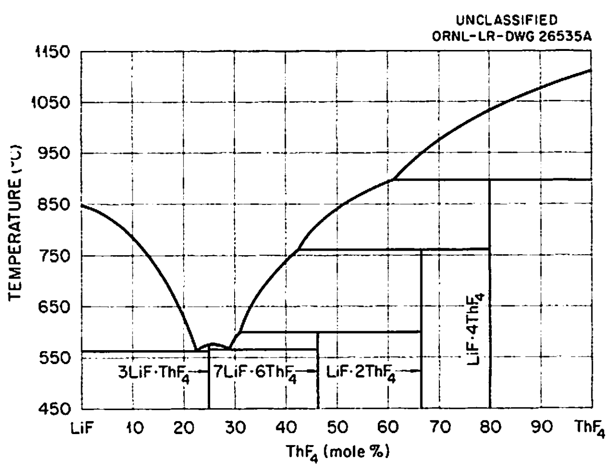

Fig. 4. The System $LiF-ThF_4$.

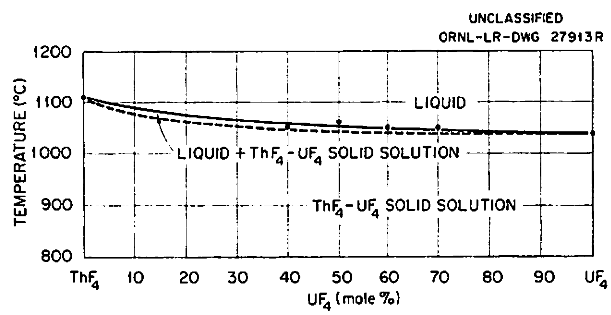

Fig. 5. The System ThF_4-UF_4.

compounds are shown in Tables 1 and 2, respectively. The compound $4LiF \cdot UF_4$ has a lower limit of stability at 470°C. The compositions and temperatures of the three peritectic invariant points and the eutectic invariant point are (1) peritectic: 26 mole % UF_4, 500°C; (2) eutectic: 27 mole % UF_4, 490°C; (3) peritectic: 40 mole % UF_4, 610°C; (4) peritectic: 57 mole % UF_4, 775°C.

One congruently melting compound ($3LiF \cdot ThF_4$) and three incongruently melting compounds ($7LiF \cdot 6ThF_4$, $LiF \cdot 2ThF_4$, and $LiF \cdot 4ThF_4$) are formed in the system LiF-ThF_4. Optical properties and x-ray diffraction data for these compounds are shown in Tables 1 and 2, respectively. The compositions and temperatures of the three peritectic and two eutectic invariant points and one congruent melting point are (1) eutectic: 23 mole % ThF_4, 565°C; (2) congruent melting point: 25 mole % ThF_4, 573°C; (3) eutectic: 29 mole % ThF_4, 568°C; (4) peritectic: 30.5 mole % ThF_4, 597°C; (5) peritectic: 42 mole % ThF_4, 762°C; (6) peritectic: 58 mole % ThF_4, 897°C.

A complete series of solid solutions without maximum or minimum is formed in the system UF_4-ThF_4. The optical properties of these solid solutions are shown in Table 1 and Fig. 6. The

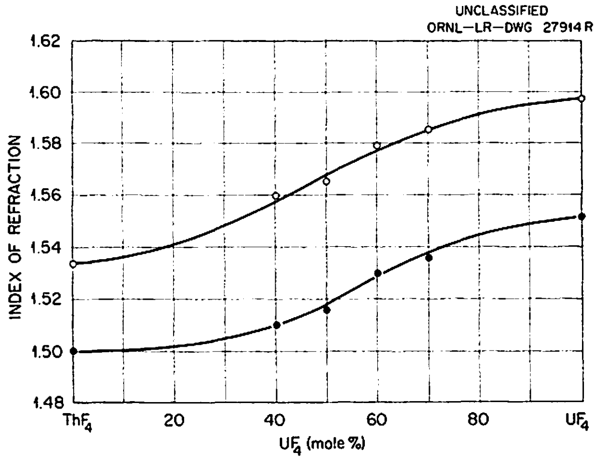

Fig. 6. Indices of Refraction vs Composition for ThF_4-UF_4 (ss).

Table 1. Optical Properties of LiF-UF_4, LiF-ThF_4, and UF_4-ThF_4 Solid Phases[a]

Compound	Optical Character	Sign	Optic Angle	N_ω or N_α	N_ϵ or N_γ
$4LiF \cdot UF_4$	Biaxial	+	45°	1.460	1.472
$7LiF \cdot 6UF_4$	Uniaxial	–		1.554	1.551
$LiF \cdot 4UF_4$	Biaxial	–	10°	1.584	1.600
$3LiF \cdot ThF_4$[b]	Biaxial	–	10°	1.480	1.488
$7LiF \cdot 6ThF_4$	Uniaxial	+		1.502	1.508
$LiF \cdot 2ThF_4$	Uniaxial	–		1.554	1.548
$LiF \cdot 4ThF_4$[b]	Biaxial	–	10°	1.528	1.538
UF_4-ThF_4 (ss[c])					
(70% UF_4)	Biaxial	–	60°	1.536	1.586
(60% UF_4)	Biaxial	–	60°	1.530	1.580
(50% UF_4)	Biaxial	–	60°	1.516	1.566
(40% UF_4)	Biaxial	–	60°	1.510	1.560

[a] Data taken from R. E. Thoma *et al.*, "Phase Equilibria in the Fused Salt Systems LiF-ThF_4 and NaF-ThF_4," *J. Phys. Chem.* (in press); H. Insley *et al.*, *Optical Properties and X-Ray Diffraction Data for Some Inorganic Fluoride and Chloride Compounds*, ORNL-2192 (Oct. 23, 1956); and L. A. Harris, G. D. White, and R. E. Thoma, "Analysis of the Solid Phases in the System LiF-ThF_4," *J. Phys. Chem.* (in press).

[b] This routinely observed biaxiality appears to be produced by strain in the $3LiF \cdot ThF_4$ and $LiF \cdot 4ThF_4$ crystals, inasmuch as the crystal type is tetragonal as determined by x-ray diffraction measurements.

[c] Solid solution.

Table 2. X-Ray Diffraction Patterns for the Solid Phases Occurring in the Systems LiF-ThF_4 and LiF-UF_4*

3LiF·ThF_4		7LiF·6ThF_4		LiF·2ThF_4		LiF·4ThF_4		4LiF·UF_4		3LiF·UF_4		7LiF·6UF_4		LiF·4UF_4	
d(Å)	I/I_1	d(Å)	I/I_1	d(Å)	I/I_1	d(Å)	I/I_1	d(Å)	I/I_1	d(Å)	I/I_1	d(Å)	I/I_1	d(Å)	I/I_1
6.42	100	6.07	15	7.97	5	8.34	3	5.67	20	4.98	20	6.61	6	7.02	8
4.46	100	5.91	20	6.37	10	7.76	3	5.46	25	4.80	15	5.97	20	6.33	12
4.37	100	5.36	90	3.96	100	6.51	5	5.13	70	4.41	100	5.82	15	6.07	5
3.62	85	5.25	15	3.57	65	5.80	25	4.93	100	4.34	100	5.24	90	5.73	25
3.09	55	4.95	30	3.25	5	4.62	5	4.55	45	3.98	15	5.15	10	4.98	8
2.866	70	4.85	20	3.21	5	4.33	70	4.44	100	3.91	8	4.65	10	4.70	25
2.788	30	4.75	100	2.97	20	3.88	100	4.23	7	3.60	80	4.37	13	4.25	90
2.542	25	4.01	85	2.822	25	3.60	60	3.82	40	3.40	10	3.95	55	3.88	20
2.327	10	3.92	15	2.675	7	3.25	10	3.55	30	3.14	25	3.85	13	3.78	100
2.189	20	3.74	15	2.528	10	2.92	25	3.03	50	3.07	50	3.68	20	3.52	90
2.104	65	3.55	65	2.388	5	2.822	25	2.89	25	2.84	80	3.49	75	3.16	8
2.071	25	3.44	10	2.123	85	2.603	10	2.866	30	2.771	30	3.33	90	3.13	8
2.036	40	3.39	70	2.053	30	2.398	10	2.747	50	2.529	35	3.15	70	3.06	12
1.959	30	3.29	60	2.001	65	2.137	25	2.468	40	2.169	15	3.07	10	2.84	40
1.933	60	3.03	100	1.787	7	2.053	35	2.398	20	2.083	75	2.99	95	2.771	55
1.877	25	2.814	25	1.701	10	2.040	10	2.221	40	2.055	35	2.771	30	2.542	8
1.771	25	2.747	25	1.689	5	2.018	10	2.167	75	1.943	50	2.707	30	2.350	10
1.743	30	2.578	20	1.603	5	2.005	30	2.074	20	1.913	25	2.542	25	2.310	10
1.701	35	2.430	10	1.519	5	1.937	20	2.025	20	1.861	30	2.350	13	2.226	8
1.661	10	2.392	10			1.820	20	1.872	20	1.751	25	2.286	25	2.000	10
1.618	10	2.302	20			1.778	3	1.836	25	1.723	25	2.264	13	2.088	35
1.547	35	2.137	20			1.725	5			1.685	25	2.184	10	2.016	60
1.520	35	2.018	5			1.719	5			1.662	8	2.097	30	1.991	50
		2.001	15			1.666	5			1.646	20	2.060	30	1.888	20
		1.892	55			1.605	5			1.599	8	2.047	75	1.819	8
		1.859	15			1.595	5					1.993	25	1.767	25
		1.804	15			1.563	5					1.972	20		
		1.680	15									1.947	25		
		1.653	20									1.924	15		
		1.600	20									1.909	30		
												1.854	45		
												1.825	20		
												1.773	20		
												1.757	25		
												1.709	15		
												1.680	15		
												1.625	15		
												1.579	25		
												1.562	8		

*Data taken from R. E. Thoma *et al.*, "Phase Equilibrium in the Fused Salt Systems LiF-ThF_4 and NaF-ThF_4," *J. Phys. Chem.* (in press); H. Insley *et al.*, *Optical Properties and X-Ray Diffraction Data for Some Inorganic Fluoride and Chloride Compounds*, ORNL-2192 (Oct. 23, 1956); L. A. Harris, G. D. White, and R. E. Thoma, "Analysis of the Solid Phases in the System LiF-ThF_4," *J. Phys. Chem.* (in press); and L. A. Harris, *Crystal Structures of 7:6 Type Compounds of Alkali Fluorides with Uranium Tetrafluoride*, ORNL CF-58-3-15 (March 6, 1958).

equilibrium phase diagram is based on the thermal analysis data shown in Table 3 and the results of quenching studies shown in Table 4.

The system LiF-UF_4-ThF_4 contains no ternary compounds but does contain four ternary solid solutions. The compounds LiF·4ThF_4–LiF·4UF_4 form a continuous series of solid solutions, as do the compounds 7LiF·6ThF_4–7LiF·6UF_4. A series of solid solutions exists having compositions at 33⅓ mole % LiF between LiF·2ThF_4 and 23 mole % UF_4. Another series of solid solutions exists having compositions at 75% LiF between 3LiF·ThF_4 and 15.5 mole % UF_4. The joins containing these solid solutions are described in detail in sections below.

Seven primary-phase fields appear in the system: LiF, 4LiF·UF_4, 3LiF·ThF_4 (ss), 7LiF·6ThF_4–7LiF·6UF_4 (ss), LiF·2ThF_4 (ss), LiF·4ThF_4–LiF·4UF_4 (ss), and ThF_4-UF_4 (ss). Phase relations were established from the liquidus to about 300°C. Three invariant points occur: peritectic: 20.5 mole % UF_4, 7 mole % ThF_4, 500°C; eutectic: 26.5 mole % UF_4, 1.5 mole % ThF_4, 488°C; peritectic: 19 mole % UF_4, 18 mole % ThF_4, 609°C. The reactions which take place at

Table 3. Thermal Analysis Data for the Systems UF_4-ThF_4 and LiF-ThF_4-UF_4*

Interpretation Key

l = liquidus
a = boundary between UF_4-ThF_4 (ss) and LiF•4UF_4–LiF•4ThF_4 (ss) primary-phase fields
b = 4LiF•UF_4 decomposition
c = boundary between LiF•2ThF_4 (ss) and LiF•4UF_4–LiF•4ThF_4 (ss) primary-phase fields
d = ternary eutectic
e = LiF, 3LiF•ThF_4 (ss), 7LiF•6UF_4–7LiF•6ThF_4 (ss) peritectic
f = boundary between 3LiF•ThF_4 (ss) and 7LiF•6UF_4–7LiF•6ThF_4 (ss) primary-phase fields
g = boundary between LiF and 7LiF•6UF_4–7LiF•6ThF_4 (ss) primary-phase fields
h = liquid disappearance at f
j = 3LiF•ThF_4 (ss) exsolution
k = liquid disappearance at m
m = boundary between LiF and 3LiF•ThF_4 (ss) primary-phase fields
s = solidus

Composition (mole %)	Temperature (°C)	Interpretation	Composition (mole %)	Temperature (°C)	Interpretation
UF_4-ThF_4**			LiF-ThF_4-UF_4		
70-30	1025		20-10-70	747	
	1023			750	
	1005		20-20-60	965	l
	985			951	l
60-40	1051	l		780	a
	1045	l		785	a
	1010		20-30-50	982	l
	993			941	l
	955			825	a
50-50	1085	l		817	a
	1080	l	20-40-40	805	a
	1050	l		795	a
	1035		20-50-30	915	
	1017			837	a
	1005			832	a
	990			825	a
	985		20-60-20	835	a
40-60	1040	l		832	a
	1035		20-70-10	855	a
	1022			860	a
	1005		33⅓-33⅓-33⅓	859	a
	990			846	a
	960			830	a
				815	a
LiF-ThF_4-UF_4				815	a
20-10-70	962	l	33⅓-46⅔-20	478	b
	960	l		430	

*In general, more than one thermal analysis was made for each nominal composition. All the thermal breaks are listed, but it is not intended to imply that they all occurred on a single cooling curve. The variation in temperatures associated with the same phenomenon is believed to be caused by supercooling effects.

**Each of these slowly cooled melts contained only one phase according to x-ray diffraction and petrographic analysis, indicating that there is no miscibility gap in the system UF_4-ThF_4.

Table 3 (continued)

Composition (mole %)	Temperature (°C)	Interpretation
$33\frac{1}{3}$-$46\frac{2}{3}$-20	320	
	300	
$33\frac{1}{3}$-$51\frac{2}{3}$-15	890	a
	870	a
	852	a
$33\frac{1}{3}$-$56\frac{2}{3}$-10	961	l
	961	l
	875	a
	875	a
	665	c
	663	c
	960	l
	956	l
	875	a
	875	a
	695	c
	692	c
35-20-45	895	l
	893	l
	805	a
	805	a
	800	a
	799	a
	480	d
	423	
35-45-20	928	l
	928	l
	850	a
	850	a
	845	a
	845	a
40-10-50	840	l
	840	l
	777	
	777	
	475	b
	445	
40-20-40	825	l
	800	
	790	
	782	
	467	b
	428	
40-30-30	863	l
	853	l
	825	
40-30-30	823	
	470	b
	458	b
40-40-20	902	
	902	
	861	l
	860	l
	590	
	588	
	467	b
	423	
40-50-10	865	l
	860	l
	855	l
	675	c
	675	c
50-10-40	755	l
	755	l
	482	d
	480	d
	420	
	428	
50-15-35	635	
	483	d
	482	d
	430	
50-25-25	803	l
	490	d
	490	d
	451	
	442	
53.8-6.2-40	720	l
	715	l
	482	d
	450	
53.8-10-36.2	717	l
	717	l
	481	d
	445	
53.8-11.2-35	730	l
	625	
	490	d
	485	d
	441	
	430	
53.8-13.2-33	725	l

Table 3 (continued)

Composition (mole %)	Temperature (°C)	Interpretation
53.8-13.2-33	725	l
	487	d
	485	d
	436	
53.8-15-31.2	726	l
	718	l
	485	d
	455	
53.8-18.2-28	740	l
	740	l
	485	d
	485	d
	446	
53.8-23.1-23.1	773	l
	770	l
	485	d
	437	
53.8-30-16.2	766	l
	751	l
	498	e
	485	d
	468	b
53.8-36.2-10	763	l
	762	l
	517	f
	515	f
	447	
57-4-39	666	l
	663	l
	550	
	535	
	493	g
	493	g
	488	d
	480	d
57-10-33	688	l
	687	l
	491	d
	490	d
	470	b
	470	b
57-15-28	705	l
	705	l
	492	g
	487	d
	483	d
57-15-28	467	b
57-21.5-21.5	717	l
	690	
	481	d
	481	d
	458	
	458	
57-26-17	708	l
	707	l
	496	e
	495	e
	485	d
	485	d
	427	
57-28-15	733	l
	733	l
	500	e
	499	e
	480	d
	480	d
	417	
57-30-13	748	l
	748	
	515	f
	514	f
	487	d
	485	d
	422	
57-32-11	750	
	750	
	687	l
	686	l
	521	f
	521	f
58-22-20	725	l
	725	l
	490	d
	442	
58-24-18	715	l
	715	l
	495	e
	480	d
	430	
60-5-35	625	l
	620	l
	489	d

Table 3 (continued)

Composition (mole %)	Temperature (°C)	Interpretation
60-5-35	488	d
	450	
	445	
	435	
60-10-30	655	l
	655	l
	490	d
	489	d
	489	d
	475	b
	475	b
	465	
	462	
60-15-25	670	l
	670	l
	490	d
	489	d
	458	
	451	
	445	
60-20-20	678	l
	678	l
	495	g
	495	g
	490	d
	490	d
	465	b
	465	b
	458	
	445	
	445	
60-22-18	685	l
	685	l
	550	f
	495	
	492	
	485	d
	485	d
	467	b
60-25-15	710	
	657	l
	657	l
	508	e
	483	d
	470	b
60-30-10	690	l
60-30-10	685	l
	670	
	665	
	527	f
	525	f
	420	
60-35-5	726	l
	718	l
	546	f
	546	f
62-10-28	618	l
	615	l
	545	
	535	
	492	g
	491	g
	485	d
	470	b
62-20-18	650	l
	650	l
	497	
	495	
	495	
	485	d
	485	d
	440	
62-28-10	687	
	685	
	675	l
	665	l
	587	
	525	f
	410	
62-33-5	704	l
	703	l
	545	f
	543	f
64-24-12	652	
	625	
	533	f
	525	f
	525	f
	523	f
64-31-5	673	l
	669	l
	544	f

Table 3 (continued)

Composition (mole %)	Temperature (^{o}C)	Interpretation	Composition (mole %)	Temperature (^{o}C)	Interpretation
64-31-5	543	f	69-27-4	540	f
	525		69-29-2	612	
66-24-10	622			611	
	620			558	f
	567	l		557	f
	528	f	70-10-20	495	f
	523	h		495	f
	517	h		487	d
66-29-5	640	l		485	d
	640	l		477	b
	536	f		462	b
	535	f	70-20-10	544	f
	530	h		540	f
	525	h		524	h
67-26-7	615			521	h
	615			520	h
	547	f		520	h
	542	f		430	
68-17-15	592	l		415	
	592	l	70-24-6	575	l
	543	f		575	l
	530	f		549	f
	512	h		540	f
	511	h	70.5-12.5-17	500	e
	487	i		500	e
	487	i		475	b
	430			475	b
68-24-8	610			455	
	607			450	
	540	l		442	
	536	l		441	
	530	f		400	
	520	f	70.5-17-12.5	525	f
	500	e		520	f
69-4-27	490	g		515	h
	487	g		511	h
	480	d		511	h
	478	d		475	b
	472	b		471	b
	467	b		442	
	445			439	
	425		71-1-28	507	l
	420			489	d
69-27-4	604	l		475	b
	600	l		545	
	549	f	71-2-27	484	d

Table 3 (continued)

Composition (mole %)	Temperature (°C)	Interpretation	Composition (mole %)	Temperature (°C)	Interpretation
71-2-27	475	b	72-8-20	516	l
	475	b		508	l
	448			508	l
71-5-24	488	d		492	d
	485	d		490	d
	485	d		450	
	483	d	72-10-18	560	
	452			500	e
	442			475	b
	440			428	
	435		72-11-17	512	l
71-24-5	560	l		501	e
	558	l		500	e
	545	h		461	b
	544	h		456	
	535	h	72-12-16	517	l
71.5-1-27.5	484	d		515	l
	484	d		508	l
	470	b		489	d
	455			485	d
71.5-2-26.5	504			441	
	487	d		428	
	475	b	72-18-10	530	l
	467	b		527	l
	451			472	b
72-1-27	762			425	
	469	b	72.5-1-26.5	480	d
	467	b		475	d
	463	b		467	b
72-2-26	475	b		467	b
	475	b		450	
	450		73-2-25	485	d
	430			476	b
72-3-25	658			475	b
	484	d		433	
	475	b	73-11-16	517	l
	462	b		511	f
	444			500	e
	428			484	d
72-4-24	504			482	d
	490	d		469	b
	487	d		460	b
	445		73-12-15	514	l
72-6-22	487	d		503	e
	482	d		477	
	480	d		477	

Table 3 (continued)

Composition (mole %)	Temperature (°C)	Interpretation	Composition (mole %)	Temperature (°C)	Interpretation
73-12-15	460		75-15-10	535	l
	439			525	m
	415			525	m
	412		75-20-5	555	l
73-15-12	517	l		555	l
	515	l		550	l
	510	f	75-23-2	803	
	507	f		563	l
	505	e		532	s
	390		77-15-8	645	
74-20-6	535	f		546	l
	535	f		545	l
74-24-2	555	f		540	k
	553	f		538	k
	465	j	77-19-4	575	
	460	i		575	
75-5-20	535			550	l
	528	l		550	l
	526	l		538	k
	489	d	80-10-10	755	
	487	d		748	
	445			493	i
	431			490	i
75-10-15	535	l		428	
	527	l	80-15-5	625	l
	512	k		625	l
	507	k		541	k
	442			541	k
	432			430	
75-12-13	524	l		420	
	521	l		415	
75-15-10	740				

Table 4. Thermal-Gradient Quenching Results for the ThF_4-UF_4 Liquidus and the LiF-ThF_4-UF_4 Liquidus[a]

Composition (mole %)	Liquidus Temperature (°C)	Primary Phase
UF_4-ThF_4		
40-60	1053 ± 4	UF_4-ThF_4 (ss[b])
50-50	1062 ± 3	UF_4-ThF_4 (ss)
60-40	1053 ± 4	UF_4-ThF_4 (ss)
70-30	1053 ± 4	UF_4-ThF_4 (ss)
UF_4-ThF_4-LiF		
2-23-75	572 ± 3	3LiF·ThF_4 (ss)
2-24-74	562 ± 3	3LiF·ThF_4 (ss)
2-29-69	594 ± 3	7LiF·6ThF_4–7LiF·6UF_4 (ss)
4-19-77	567 ± 3	LiF
4-27-69	598 ± 6	7LiF·6ThF_4–7LiF·6UF_4 (ss)
5-15-80	615 ± 3	LiF
5-19-76	562 ± 2	3LiF·ThF_4 (ss)
5-20-75	562 ± 3	3LiF·ThF_4 (ss)
5-24-71	565 ± 3	7LiF·6ThF_4–7LiF·6UF_4 (ss)
22-6-72	504 ± 4	LiF
23.1-23.1-53.8	744 ± 3	LiF·4ThF_4–LiF·4UF_4 (ss)
24-4-72	495 ± 2	LiF + 7LiF·6ThF_4–7LiF·6UF_4 (ss)
25-2-73	491 ± 2	LiF + 7LiF·6ThF_4–7LiF·6UF_4 (ss)
25-3-72	495 ± 2	LiF + 7LiF·6ThF_4–7LiF·6UF_4 (ss)
25-25-50	806 ± 3	LiF·4ThF_4–LiF·4UF_4 (ss)
26-2-72	496 ± 2	LiF + 7LiF·6ThF_4–7LiF·6UF_4 (ss)[c]
26.5-1-72.5	495 ± 2	4LiF·UF_4 + 7LiF·6ThF_4–7LiF·6UF_4 (ss)
26.5-2-71.5	504 ± 2	4LiF·UF_4 + 7LiF·6ThF_4–7LiF·6UF_4 (ss)
27-1-72	491 ± 2	4LiF·UF_4 + 7LiF·6ThF_4–7LiF·6UF_4 (ss)
27-2-71	495 ± 2	LiF + 7LiF·6ThF_4–7LiF·6UF_4 (ss)
27.5-1-71.5	495 ± 2	4LiF·UF_4 + 7LiF·6ThF_4–7LiF·6UF_4 (ss)
28-1-71	508 ± 2	7LiF·6ThF_4–7LiF·6UF_4 (ss)
28-10-62	615 ± 3	LiF·4UF_4–LiF·4ThF_4 (ss)
28-18.2-53.8	729 ± 3	LiF·4UF_4–LiF·4ThF_4 (ss)
30-10-60	633 ± 2	LiF·4UF_4–LiF·4ThF_4 (ss)
30-30-40	859 ± 1	LiF·4UF_4–LiF·4ThF_4 (ss)
30-50-20	968 ± 4	UF_4-ThF_4 (ss)

Table 4 (continued)

Composition (mole %)	Liquidus Temperature (°C)	Primary Phase
UF_4-ThF_4-LiF		
31.2-15-53.8	736 ± 3	LiF•4UF_4–LiF•4ThF_4 (ss)
33-10-57	687 ± 3	LiF•4UF_4–LiF•4ThF_4 (ss)
33-13.2-53.8	723 ± 3	LiF•4UF_4–LiF•4ThF_4 (ss)
5-26-69	581 ± 2	7LiF•6ThF_4–7LiF•6UF_4
5-29-66	645 ± 3	LiF•2ThF_4 (ss)
5-31-64	667 ± 3	LiF•2ThF_4 (ss)
5-33-62	704 ± 3	LiF•2ThF_4 (ss)
5-35-60	714 ± 3	LiF•2ThF_4 (ss)
6-24-70	555 ± 2	7LiF•6ThF_4–7LiF•6UF_4 (ss)
7-26-67	612 ± 5	7LiF•6ThF_4–7LiF•6UF_4 (ss)
8-15-77	548 ± 3	LiF + 3LiF•ThF_4 (ss)
10-10-80	649 ± 3	LiF
10-15-75	547 ± 3	3LiF•ThF_4 (ss)
10-16-74	555 ± 2	3LiF•ThF_4 (ss)
10-18-72	544 ± 2	3LiF•ThF_4 (ss) + 7LiF•6ThF_4–7LiF•6UF_4 (ss)
10-20-70	577 ± 9	7LiF•6ThF_4–7LiF•6UF_4 (ss)
10-24-66	596 ± 3	7LiF•6ThF_4–7LiF•6UF_4 (ss)
10-26-64	600 ± 3	7LiF•6ThF_4–7LiF•6UF_4 (ss)
10-36.2-53.8	770 ± 3	LiF•4ThF_4–LiF•4UF_4 (ss)
	772 ± 2	LiF•4ThF_4–LiF•4UF_4 (ss)
10-50-40	880 ± 2	LiF•4ThF_4–LiF•4UF_4 (ss)
10-70-20	1013 ± 6	UF_4-ThF_4 (ss)
12-15-73	533 ± 3	3LiF•ThF_4 (ss)
12.5-17-70.5	565 ± 3	7LiF•6ThF_4–7LiF•6UF_4 (ss)
13-12-75	528 ± 3	3LiF•ThF_4 (ss)
15-12-73	523 ± 2	LiF + 3LiF•ThF_4 (ss)
	528 ± 3	LiF + 3LiF•ThF_4 (ss)
15-17-68	587 ± 2	7LiF•6ThF_4–7LiF•6UF_4 (ss)
16-11-73	519 ± 2	3LiF•ThF_4 (ss)
16-12-72	528 ± 3	7LiF•6ThF_4–7LiF•6UF_4 (ss)
16.2-30-63.8	777 ± 3	LiF•4ThF_4–LiF•4UF_4 (ss)
17-11-72	532 ± 2	7LiF•6ThF_4–7LiF•6UF_4 (ss) + 3LiF•ThF_4 (ss)
17-12.5-70.5	547 ± 3	7LiF•6ThF_4–7LiF•6UF_4 (ss)

Table 4 (continued)

Composition (mole %)	Liquidus Temperature (°C)	Primary Phase
UF_4-ThF_4-LiF		
18-10-72	511 ± 2	3LiF·ThF_4 (ss)
18-18-64	612 ± 4	7LiF·6ThF_4–7LiF·6UF_4 (ss)
18-20-62	634 ± 4	LiF·2ThF_4 (ss)[c]
18-22-60	680 ± 3	LiF·4ThF_4–LiF·4UF_4 (ss)
20-8-72	508 ± 2	3LiF·ThF_4 (ss)[c]
20-20-60	637 ± 2	LiF·4ThF_4–LiF·4UF_4 (ss)
20-40-40	862 ± 3	LiF·4ThF_4–LiF·4UF_4 (ss)
20-45-35	892 ± 2	UF_4-ThF_4 (ss)
20-60-20	1011 ± 3	UF_4-ThF_4 (ss)
21.5-21.5-57	736 ± 2	LiF·4ThF_4–LiF·4UF_4 (ss)
35-5-60	630 ± 3	LiF·4UF_4–LiF·4ThF_4 (ss)
35-11.2-53.8	729 ± 3	LiF·4UF_4–LiF·4ThF_4 (ss)
35-15-50	780 ± 3	LiF·4UF_4–LiF·4ThF_4 (ss)
39-4-57	625 ± 2	LiF·4UF_4–LiF·4ThF_4 (ss)
40-6.2-53.8	717 ± 3	LiF·4UF_4–LiF·4ThF_4 (ss)
40-10-50	767 ± 4	LiF·4UF_4–LiF·4ThF_4 (ss)
40-20-40	829 ± 4	LiF·4UF_4–LiF·4ThF_4 (ss)
40-40-20	972 ± 3	UF_4-ThF_4 (ss)
50-10-40	808 ± 3	LiF·4UF_4–LiF·4ThF_4 (ss)
50-30-20	968 ± 4	UF_4-ThF_4 (ss)
60-20-20	960 ± 2	UF_4·ThF_4 (ss)
70-10-20	963 ± 3	UF_4·ThF_4 (ss)

[a] The uncertainty in temperatures in this table indicates the temperature differences between the quenched samples.

[b] Solid solution.

[c] Most of the phases were identified by optical microscopy; in addition, this phase was identified by x-ray diffraction.

these invariant points are the following:

The peritectic at 609°C ·

LiF·4UF_4–LiF·4ThF_4 (ss) + liquid $\rightleftharpoons$
7LiF·6 ThF_4–7LiF·6UF_4 (ss) + LiF·2ThF_4 (ss)

The peritectic at 500°C

3LiF·ThF_4 (ss) + liquid $\rightleftharpoons$
7LiF·6UF_4–7LiF·6ThF_4 (ss) + LiF

The eutectic at 488°C

Liquid $\rightleftharpoons$ LiF + 3LiF·ThF_4 (ss) +
+ 7LiF·6UF_4–7LiF·6ThF_4 (ss)

The equilibrium phase diagram in Fig. 1 is based on the thermal analysis data shown in Table 3 and the results of quenching studies shown in Table 4 and in the appendix. The results of quenching experiments, excluding liquidus temperature and compositions, which aid in locating the invariant points and in describing the invariant reactions are shown in Table 5. The peritectic or eutectic nature of the invariant reactions is further confirmed by the construction of compatibility triangles and observing the position of these triangles relative to their invariant points.

Because this system contains several series of extensive ternary solid solutions, it cannot be completely described without knowledge of the composition of the crystalline phase or phases at equilibrium at any temperature and composition. (The phrase "ternary solid solution" as used in this report implies that the solid solution composition lies within the system $LiF\text{-}UF_4\text{-}ThF_4$.

Table 5. Invariant-Point Data[a] for the System $LiF\text{-}ThF_4\text{-}UF_4$

Quench Composition (mole %)		Temperature[b] (°C)	Phases[c] Above Temperature	Phases[c] Below Temperature
ThF_4	UF_4			
6	22	495 ± 2	Liquid + LiF	Liquid + LiF + $7LiF\cdot6UF_4$–$7LiF\cdot6ThF_4$ (ss)
		492 ± 2	Liquid + LiF + $7LiF\cdot6UF_4$–$7LiF\cdot6ThF_4$ (ss)	LiF[d] + $7LiF\cdot6UF_4$–$7LiF\cdot6ThF_4$ (ss)[d]
8	20	502 ± 2	Liquid + $3LiF\cdot ThF_4$ (ss)[d]	Liquid + $3LiF\cdot ThF_4$ (ss) + $7LiF\cdot6UF_4$–$7LiF\cdot6ThF_4$ (ss)
		498 ± 2	Liquid + $3LiF\cdot ThF_4$ (ss) + $7LiF\cdot6UF_4$–$7LiF\cdot6ThF_4$ (ss)	LiF + $3LiF\cdot ThF_4$ (ss) + $7LiF\cdot6UF_4$–$7LiF\cdot6ThF_4$ (ss)
10	18	502 ± 2	Liquid + $3LiF\cdot ThF_4$ (ss)	LiF + $3LiF\cdot ThF_4$ (ss) + $7LiF\cdot6UF_4$–$7LiF\cdot6ThF_4$ (ss)
		489 ± 2	Liquid + $3LiF\cdot ThF_4$ (ss) + $7LiF\cdot6UF_4$–$7LiF\cdot6ThF_4$ (ss)	LiF + $3LiF\cdot ThF_4$ (ss) + $7LiF\cdot6UF_4$–$7LiF\cdot6ThF_4$ (ss)
11	16	510 ± 2	Liquid + $3LiF\cdot ThF_4$ (ss)	Liquid + $3LiF\cdot ThF_4$ (ss) + $7LiF\cdot6UF_4$–$7LiF\cdot6ThF_4$ (ss)
		506 ± 2	Liquid + $3LiF\cdot ThF_4$ (ss) + $7LiF\cdot6UF_4$–$7LiF\cdot6ThF_4$ (ss)	Liquid + $3LiF\cdot ThF_4$ (ss) + $7LiF\cdot6UF_4$–$7LiF\cdot6ThF_4$ (ss) + LiF [inclusions in $3LiF\cdot ThF_4$ (ss)]
		496 ± 3	Liquid + $3LiF\cdot ThF_4$ (ss) + $7LiF\cdot6UF_4$–$7LiF\cdot6ThF_4$ (ss) + LiF [inclusions in $3LiF\cdot ThF_4$ (ss)]	Liquid + $3LiF\cdot ThF_4$ (ss) + $7LiF\cdot6UF_4$–$7LiF\cdot6ThF_4$ (ss) + LiF
		492 ± 2	Liquid + $3LiF\cdot ThF_4$ (ss) + $7LiF\cdot6UF_4$–$7LiF\cdot6ThF_4$ (ss) + LiF	$3LiF\cdot ThF_4$ (ss) + $7LiF\cdot6UF_4$–$7LiF\cdot6ThF_4$ (ss) + LiF
11	17	501 ± 3	Liquid + $7LiF\cdot6UF_4$–$7LiF\cdot6ThF_4$ (ss) + $3LiF\cdot ThF_4$ (ss)	Liquid + $7LiF\cdot6UF_4$–$7LiF\cdot6ThF_4$ (ss) + $3LiF\cdot ThF_4$ (ss) + LiF
		497 ± 3	Liquid + $7LiF\cdot6UF_4$–$7LiF\cdot6ThF_4$ (ss) + $3LiF\cdot ThF_4$ (ss) + LiF	$7LiF\cdot6UF_4$–$7LiF\cdot6ThF_4$ (ss) + $3LiF\cdot ThF_4$ (ss) + LiF
12	15	511 ± 3	Liquid + $3LiF\cdot ThF_4$ (ss)	Liquid + $7LiF\cdot6UF_4$–$7LiF\cdot6ThF_4$ (ss) + $3LiF\cdot ThF_4$ (ss)
		502 ± 3	Liquid + $7LiF\cdot6UF_4$–$7LiF\cdot6ThF_4$ (ss) + $3LiF\cdot ThF_4$ (ss)	$7LiF\cdot6UF_4$–$7LiF\cdot6ThF_4$ (ss) + $3LiF\cdot ThF_4$ (ss) + LiF

Table 5 (continued)

Quench Composition (mole %)		Temperature[b] (°C)	Phases[c] Above Temperature	Phases[c] Below Temperature
ThF_4	UF_4			
12	16	523 ± 2	Liquid + $7LiF \cdot 6UF_4$–$7LiF \cdot 6ThF_4$ (ss)	Liquid + $7LiF \cdot 6UF_4$–$7LiF \cdot 6ThF_4$ (ss) + $3LiF \cdot ThF_4$ (ss)
		504 ± 3	Liquid + $7LiF \cdot 6UF_4$–$7LiF \cdot 6ThF_4$ (ss) + $3LiF \cdot ThF_4$ (ss)	$7LiF \cdot 6UF_4$–$7LiF \cdot 6ThF_4$ (ss) + LiF
1	26.5	490 ± 3	Liquid + $4LiF \cdot UF_4$ + $7LiF \cdot 6UF_4$–$7LiF \cdot 6ThF_4$ (ss)	$4LiF \cdot UF_4$ + $7LiF \cdot 6UF_4$–$7LiF \cdot 6ThF_4$ (ss) + LiF
1	27	487 ± 2	Liquid + $4LiF \cdot UF_4$ + $7LiF \cdot 6UF_4$–$7LiF \cdot 6ThF_4$ (ss)	$4LiF \cdot UF_4$ + $7LiF \cdot 6UF_4$–$7LiF \cdot 6ThF_4$ (ss) + LiF
1	27.5	485 ± 3	$4LiF \cdot UF_4$ + $7LiF \cdot 6UF_4$–$7LiF \cdot 6ThF_4$ (ss)	$4LiF \cdot UF_4$ + $7LiF \cdot 6UF_4$–$7LiF \cdot 6ThF_4$ (ss) + LiF
1	28	490 ± 3	Liquid + $7LiF \cdot 6UF_4$–$7LiF \cdot 6ThF_4$ (ss)	$4LiF \cdot UF_4$ + $7LiF \cdot 6UF_4$–$7LiF \cdot 6ThF_4$ (ss) + LiF(?) + liquid(?)
		485 ± 3	$7LiF \cdot 6UF_4$–$7LiF \cdot 6ThF_4$ (ss) + $4LiF \cdot UF_4$ + LiF(?) + liquid(?)	$7LiF \cdot 6UF_4$–$7LiF \cdot 6ThF_4$ (ss) + $4LiF \cdot UF_4$ + LiF
24	18	640 ± 3	Liquid + $LiF \cdot 4UF_4$–$LiF \cdot 4ThF_4$ (ss)[d]	Liquid + $LiF \cdot 2ThF_4$ (ss)[d]
		615 ± 4	Liquid + $LiF \cdot 2ThF_4$ (ss)[d]	Liquid + $7LiF \cdot 6UF_4$–$7LiF \cdot 6ThF_4$ (ss)[d]
22	20	615 ± 4	Liquid + $LiF \cdot 4UF_4$–$LiF \cdot 4ThF_4$ (ss)[d]	Liquid + $7LiF \cdot 6UF_4$–$7LiF \cdot 6ThF_4$ (ss)[d]

[a]For liquidus data near invariant points see Table 4.

[b]The uncertainty in temperatures indicates the temperature differences between the quenched samples.

[c]Only phases found in major quantity are given. Minor quantities of other phases resulting from lack of complete reaction between solids or from trace amounts of oxide impurities are not noted. Glasses or poorly formed crystals assumed to have been produced during rapid cooling of liquid were found in those samples for which the observed phase is indicated as "liquid."

[d]Most of the phases were identified by optical microscopy. In addition, this phase was identified by x-ray diffraction.

Each of the solid solutions in this system, however, may be formed from mixtures of two end members and in this sense form a binary series.) In general, in any series of complete solid solution the physical properties (e.g., density, optical properties, x-ray diffraction patterns, etc.) of the individual members show a continuous change between those of the end members. Hence a determination of refractive indices of a number of samples of known compositions in the solid solution series provides a method of establishing in the ternary system tie lines between the composition of crystals in this solid solution series with the liquid with which it is in equilibrium. In the case of the system LiF-ThF_4-UF_4 the determination of refractive indices of the members of each of the four ternary solid solution series present provides a particularly good method of establishing tie lines, because the refractive indices of the end members of each series are so different that a good degree of precision can be obtained.

Once the tie lines are established for a primary-phase area, the fractionation paths may be drawn. Fractionation paths in four of the primary-phase areas of system LiF-UF_4-ThF_4 are shown in

Fig. 7. The compounds LiF and $4LiF \cdot UF_4$ do not form solid solutions. Consequently, the tie lines, equilibrium paths, and fractionation paths for their primary-phase areas can be drawn directly from Fig. 1, and the case is trivial. The fractionation paths for the UF_4-ThF_4 (ss) primary-phase area cannot be drawn from Fig. 1. From Fig. 6 it can be seen that the indices of refraction for UF_4-ThF_4 (ss) do not always change rapidly enough with respect to composition to allow a high degree of precision in tie-line determinations. Consequently, no attempt was made to determine the fractionation paths in this primary-phase area.

THE 20 MOLE % LiF JOIN AND THE $LiF \cdot 4UF_4$–$LiF \cdot 4ThF_4$ (ss) FRACTIONATION PATHS

A diagram of the 20 mole % LiF join is shown in Fig. 8 and is based on the thermal analysis data in Table 3 and the results of quenching studies in Tables 4, 6, and 7. The join contains the $LiF \cdot 4UF_4$–$LiF \cdot 4ThF_4$ (ss) series, whose members are green, are biaxial negative, and have optic angles of approximately 10°. The indices of refraction of these solid solutions shown in Fig. 9 and Table 8 vary almost linearly with UF_4 concentration.

UNCLASSIFIED
ORNL-LR-DWG 35505R

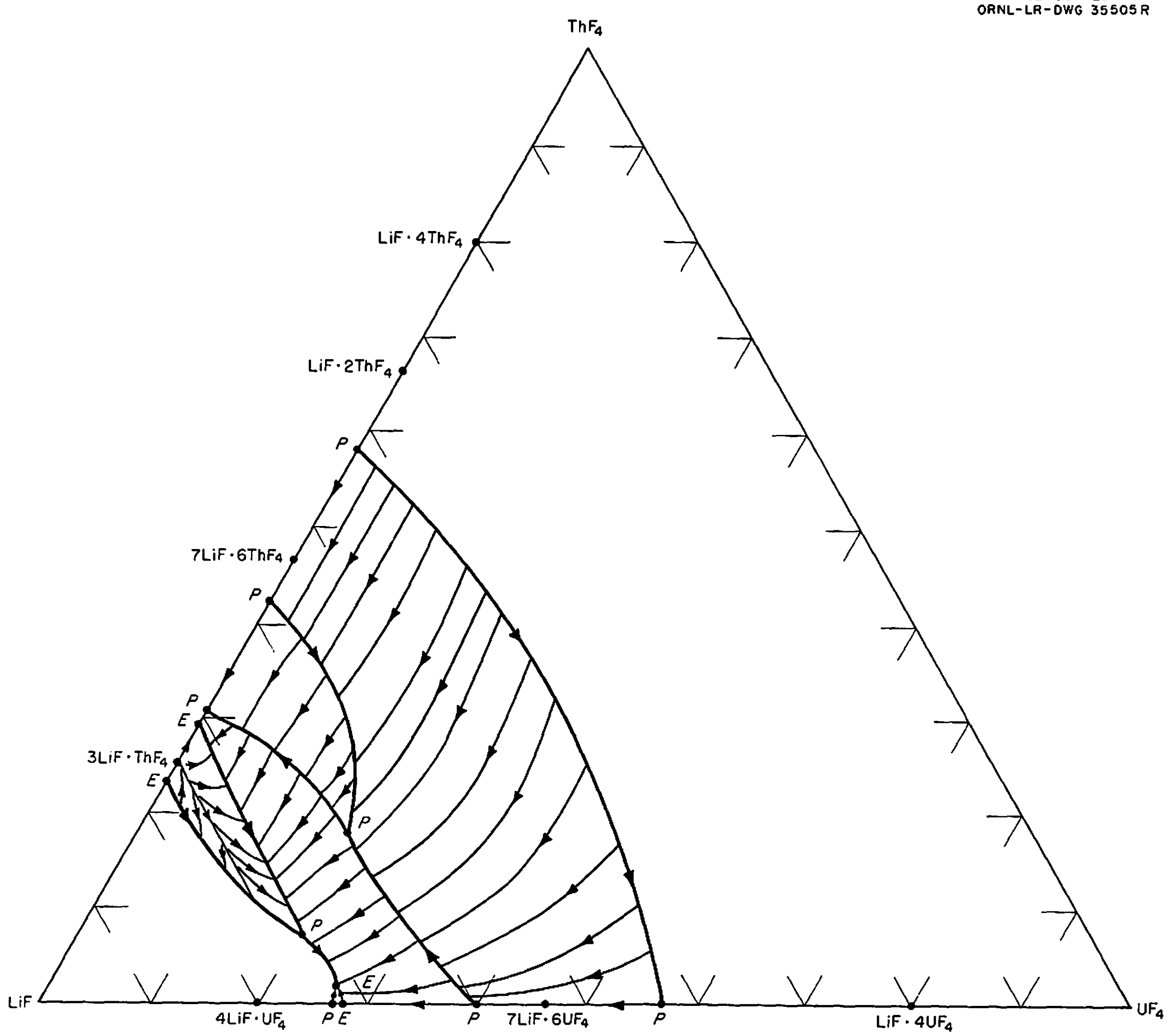

Fig. 7. Fractionation Paths.

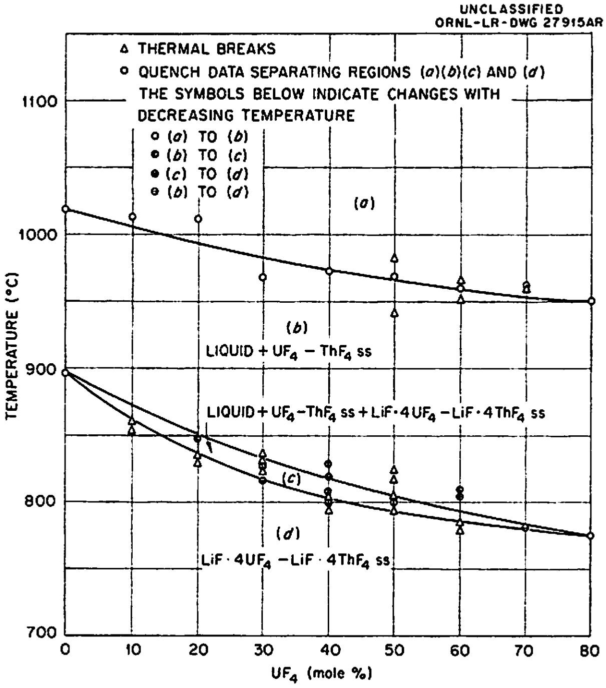

Fig. 8. The Join $LiF{\cdot}4UF_4$–$LiF{\cdot}4ThF_4$.

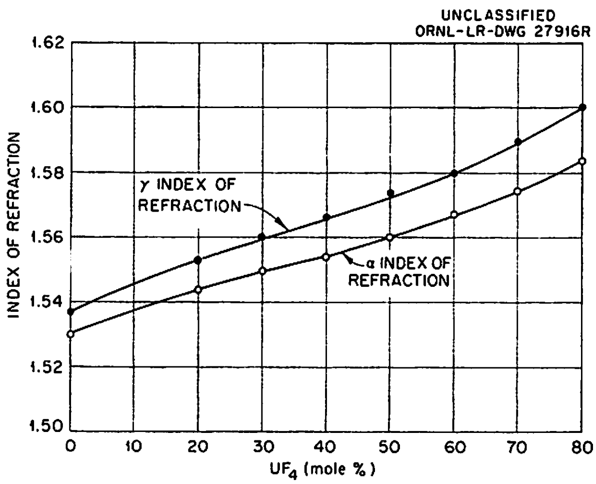

Fig. 9. Indices of Refraction vs Composition for $LiF{\cdot}4UF_4$–$LiF{\cdot}4ThF_4$ (ss).

The fractionation paths for the $LiF{\cdot}4UF_4$–$LiF{\cdot}4ThF_4$ (ss) primary-phase area shown in Fig. 7 are based on the tie-line data in Table 7. They tend to parallel the system LiF-ThF_4 over most of the $LiF{\cdot}4UF_4$–$LiF{\cdot}4ThF_4$ (ss) primary-phase area, and they change from this pattern only at the higher UF_4 concentrations.

THE $33\frac{1}{3}$ MOLE % LiF JOIN AND THE $LiF{\cdot}2Th(U)F_4$ (ss) FRACTIONATION PATHS

A diagram of the $33\frac{1}{3}$ mole % LiF join is shown in Fig. 10 and is based on the thermal analysis data in Table 3 and the results of quenching studies in Tables 4, 9, and 10. The join contains the $LiF{\cdot}2Th(U)F_4$ (ss) series, whose members are green and are uniaxial negative. The indices of refraction of these solid solutions shown in Fig. 11 and Table 11 vary linearly with UF_4 concentration. The maximum extent of $LiF{\cdot}2Th(U)F_4$ (ss) at the solidus is 23 mole % UF_4.

The fractionation paths for $LiF{\cdot}2Th(U)F_4$ (ss) primary-phase area shown in Fig. 7 are based on the tie-line data in Table 10. The fractionation paths tend to parallel the system LiF-ThF_4 over the entire primary-phase area.

THE 53.8 MOLE % LiF JOIN AND THE $7LiF{\cdot}6UF_4$–$7LiF{\cdot}6ThF_4$ (ss) FRACTIONATION PATHS

A diagram of the 53.8 mole % LiF join is shown in Fig. 12 and is based on thermal analysis data in Table 3 and the results of quenching studies in Tables 4, 12, and 13. The join contains the $7LiF{\cdot}6UF_4$–$7LiF{\cdot}6ThF_4$ (ss) series, whose members are green and are uniaxial. Their indices of refraction, shown in Fig. 13 and Table 14, vary linearly with UF_4 concentration. There should be one composition which is practically isotropic, since the ordinary and extraordinary indices of refraction cross. Actually there is a range of compositions in the midportion of the series which have a birefringence too low to be observed.

The fractionation paths for the $7LiF{\cdot}6ThF_4$–$7LiF{\cdot}6UF_4$ primary-phase area shown in Fig. 7 are based on the tie-line data in Table 13. They parallel the system LiF-ThF_4 over most of the $7LiF{\cdot}6UF_4$–$7LiF{\cdot}6ThF_4$ primary-phase area and change from this pattern only at the higher UF_4 concentrations.

THE 75 MOLE % LiF JOIN AND THE $3LiF{\cdot}ThF_4$ (ss) FRACTIONATION PATHS

A diagram of the 75 mole % LiF join is shown in Fig. 14 and is based on the thermal analysis data in Table 3 and the results of quenching

Table 6. Thermal-Gradient Quenching Data for 20 Mole % LiF Join[a]

UF_4 Content (mole %)	Temperature[b] (°C)	Phases[c] Above Temperature	Phases[c] Below Temperature
20	849 ± 3	Liquid + UF_4-ThF_4 (ss)[d]	Liquid + LiF·4UF_4–LiF·4ThF_4 (ss)[d] + UF_4-ThF_4 (ss)[d]
30	827 ± 3	Liquid + UF_4-ThF_4 (ss)	Liquid + LiF·4UF_4–LiF·4ThF_4 (ss) + UF_4-ThF_4 (ss)
	816 ± 6	Liquid + UF_4-ThF_4 (ss) + LiF·4UF_4–LiF·4ThF_4 (ss)	LiF·4UF_4–LiF·4ThF_4 (ss)
40	830 ± 3	Liquid + UF_4-ThF_4 (ss)	Liquid + LiF·4UF_4–LiF·4ThF_4 (ss) + UF_4-ThF_4 (ss)
	820 ± 3	Liquid + LiF·4UF_4–LiF·4ThF_4 (ss) + UF_4-ThF_4 (ss)	LiF·4UF_4–LiF·4ThF_4 (ss)
	809 ± 5	Liquid + UF_4-ThF_4 (ss)	Liquid + UF_4-ThF_4 (ss) + LiF·4UF_4–LiF·4ThF_4 (ss)
	800 ± 5	Liquid + UF_4-ThF_4 (ss)[d] + LiF·4UF_4–LiF·4ThF_4 (ss)[d]	LiF·4UF_4–LiF·4ThF_4 (ss)[d]
50	800 ± 4	Liquid + UF_4-ThF_4 (ss)[d]	Liquid + UF_4-ThF_4 (ss) + LiF·4UF_4–LiF·4ThF_4 (ss)
60	811 ± 4	Liquid + UF_4-ThF_4 (ss)	Liquid + UF_4-ThF_4 (ss) + LiF·4UF_4–LiF·4ThF_4 (ss)
	805 ± 4	Liquid + UF_4-ThF_4 (ss) + LiF·4UF_4–LiF·4ThF_4 (ss)	LiF·4UF_4–LiF·4ThF_4 (ss)[d]
70	782 ± 2	Liquid + UF_4-ThF_4 (ss)	LiF·4UF_4–LiF·4ThF_4 (ss)

[a]See Table 4 for liquidus values.

[b]The uncertainty in temperatures in this table indicates the temperature differences between the quenched samples.

[c]Only phases found in major quantity are given. Minor quantities of other phases resulting from lack of complete reaction between solids or from trace amounts of oxide impurities are not noted. Glasses or poorly formed crystals assumed to have been produced during rapid cooling of liquid were found in those samples for which the observed phase is indicated as "liquid."

[d]Most of the phases were identified by optical microscopy; this phase was also identified by x-ray diffraction.

Table 7. Tie-Line Data for $LiF \cdot 4UF_4$–$LiF \cdot 4ThF_4$ (ss) Primary-Phase Area

Quench Composition (mole %)		Temperature Range (°C)	Index of Refraction, N_γ	Solid Solution Composition (mole % UF_4)
UF_4	ThF_4			
5	61⅔	729–801	1.541	5
10	36.2	695–765	1.548	13
10	50	753–879	1.544	8
10	56⅔	708–801	1.546	10
13	30	690–700	1.550	15.5
15	28	683–700	1.550	15.5
15	51⅔	670–735	1.548	13
16.2	30	648–651	1.556	24.5
		646–763	1.554	21.5
17	26	663–700	1.552	18.5
18	24	643–658	1.554	21.5
20	20	635	1.558	28
20	22	619–658	1.556	24.5
20	40	860	1.548	13
		741	1.552	18
20	45	877	1.550	15.5
		734	1.554	20
20	46⅔	635–735	1.552	18
21.5	21.5	613–736	1.559	29
23.1	23.1	614	1.562	34
		620–641	1.562	34
		646	1.560	31
		686–742	1.558	28
		621–661	1.560	31
25	15	708	1.564	38
		656	1.566	41
		613	1.568	44
		651	1.564	38
		618	1.566	41
		617–635	1.564	38
25	25	804	1.558	28
		693	1.560	31
28	10	613	1.568	44
28	18.2	707	1.562	34
		700	1.562	34
		610	1.565	40
30	10	613–629	1.570	47
30	30	843	1.552	18
31.2	15	611–641	1.569	45.5
		678	1.569	45.5
		734	1.565	40
		607	1.571	48
33	10	607–684	1.574	53

Table 7 (continued)

Quench Composition (mole %)		Temperature Range (°C)	Index of Refraction, N_γ	Solid Solution Composition (mole % UF_4)
UF_4	ThF_4			
33	13.2	720	1.574	53
		610	1.572	50
33⅓	33⅓	792–860	1.560	31
35	5	623–629	1.582	63
		612–623	1.582	63
35	11.2	726	1.574	53
		610	1.576	55
35	15	763–777	1.568	44
		756	1.570	47
		693–731	1.572	50
36.2	10	641	1.575	54
		608	1.578	58
		626–674	1.578	58
39	4	614–623	1.590	71
40	6.2	714	1.580	60
		610	1.584	65
40	10	731	1.576	55
		693	1.579	59
40	20	846	1.568	44
		741	1.570	47
45	20	855	1.572	50
		734	1.574	53
50	10	781–805	1.578	58

Table 8. Refractive Indices for $LiF \cdot 4UF_4$–$LiF \cdot 4ThF_4$ (ss)

UF_4 Content (mole %)	Refractive Indices	
	N_α	N_γ
20	1.544	1.553
30	1.550	1.560
40	1.554	1.565
50	1.560	1.574
60	1.567	1.580
70	1.574	1.590

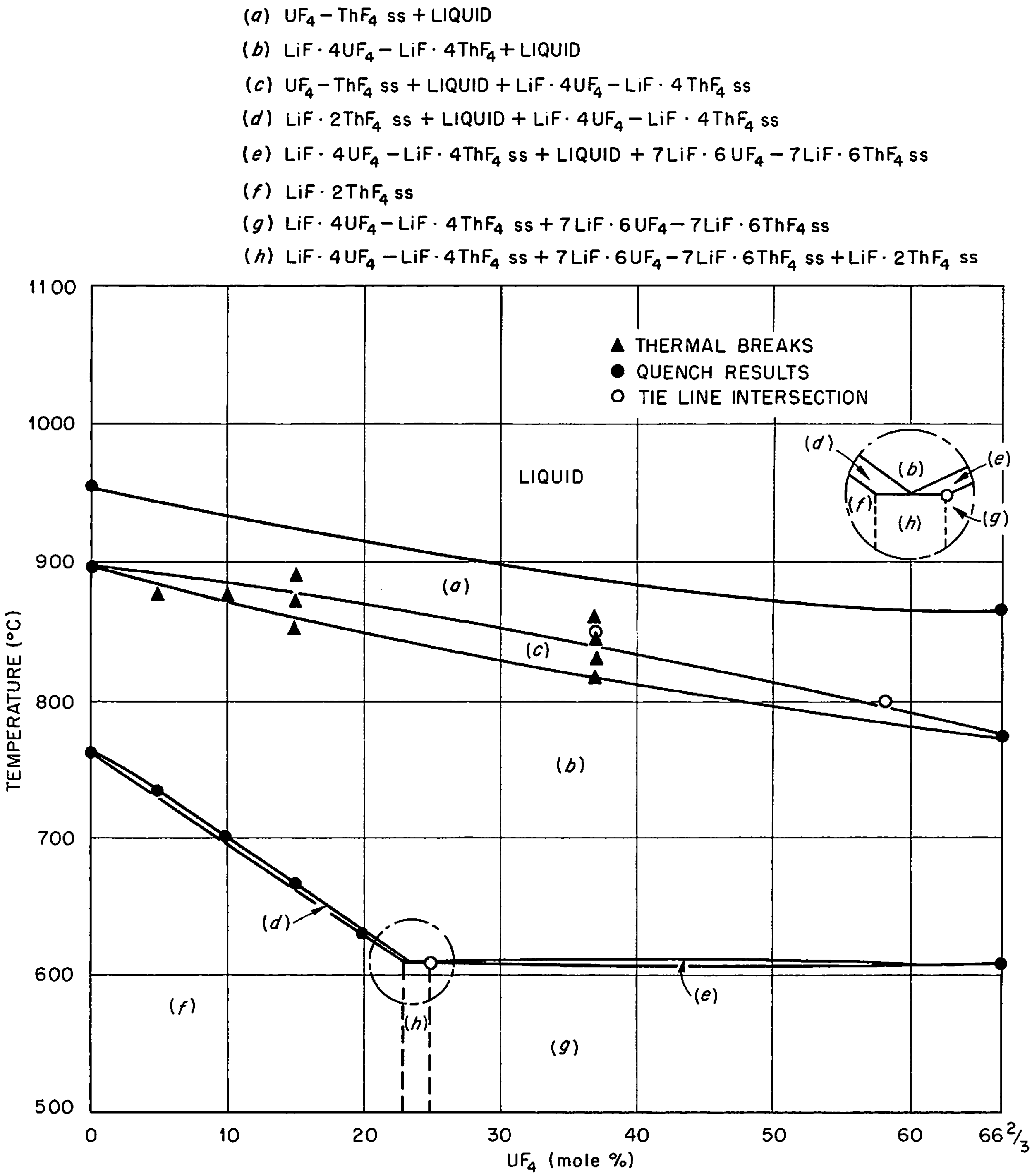

Fig. 10. The $33\frac{1}{3}$ Mole % LiF Section.

Table 9. Quench Data for $LiF \cdot 2ThF_4$ (ss)

UF_4 Content (mole %)	Temperature[a] (°C)	Phases Above[b] Temperature	Phases Below[b] Temperature
5	723 ± 4	Liquid + $LiF \cdot 4UF_4$–$LiF \cdot 4ThF_4$ (ss)[c]	$LiF \cdot 2ThF_4$ (ss)[c]
10	700 ± 4	Liquid + $LiF \cdot 4UF_4$–$LiF \cdot 4ThF_4$ (ss)[c]	$LiF \cdot 2ThF_4$ (ss)[c]
15	667 ± 4	Liquid + $LiF \cdot 4UF_4$–$LiF \cdot 4ThF_4$ (ss)[c]	$LiF \cdot 2ThF_4$ (ss)[c,d]
20	632 ± 4	Liquid + $LiF \cdot 4UF_4$–$LiF \cdot 4ThF_4$ (ss)[c]	$LiF \cdot 2ThF_4$ (ss)[c,d]

[a]The uncertainty in temperatures indicates the temperature differences between the quenched samples.

[b]Only phases found in major quantity are given. Minor quantities of other phases resulting from lack of complete reaction between solids or from trace amounts of oxide impurities are not noted. Glasses or poorly formed crystals assumed to have been produced during rapid cooling of liquid were found in those samples for which the observed phase is indicated as "liquid."

[c]Most of the phases were identified by optical microscopy; this phase was also identified by x-ray diffraction.

[d]This continues down to at least 578°C.

Table 10. Tie-Line Data for $LiF \cdot 2ThF_4$ (ss) Primary-Phase Area

Quench Composition (mole %)		Temperature Range (°C)	Index of Refraction, N_ω	Solid Solution Composition (mole % UF_4)
UF_4	ThF_4			
5	29	618	1.556	5
5	31	644	1.556	5
5	33	658–670	1.556	5
5	35	698	1.556	5
10	36.2	611–665	1.560	15
		633–695	1.560	15
11	32	615–700	1.557	7.5
13	30	615–687	1.560	15
15	25	619–658	1.559	12.5
15	28	620–678	1.561	17.5
17	28	620–657	1.560	15
18	20	616–630	1.563	23
		618–634	1.563	23
18	22	618–624	1.564	23
		618–630	1.564	23
18	24	619–637	1.562	20

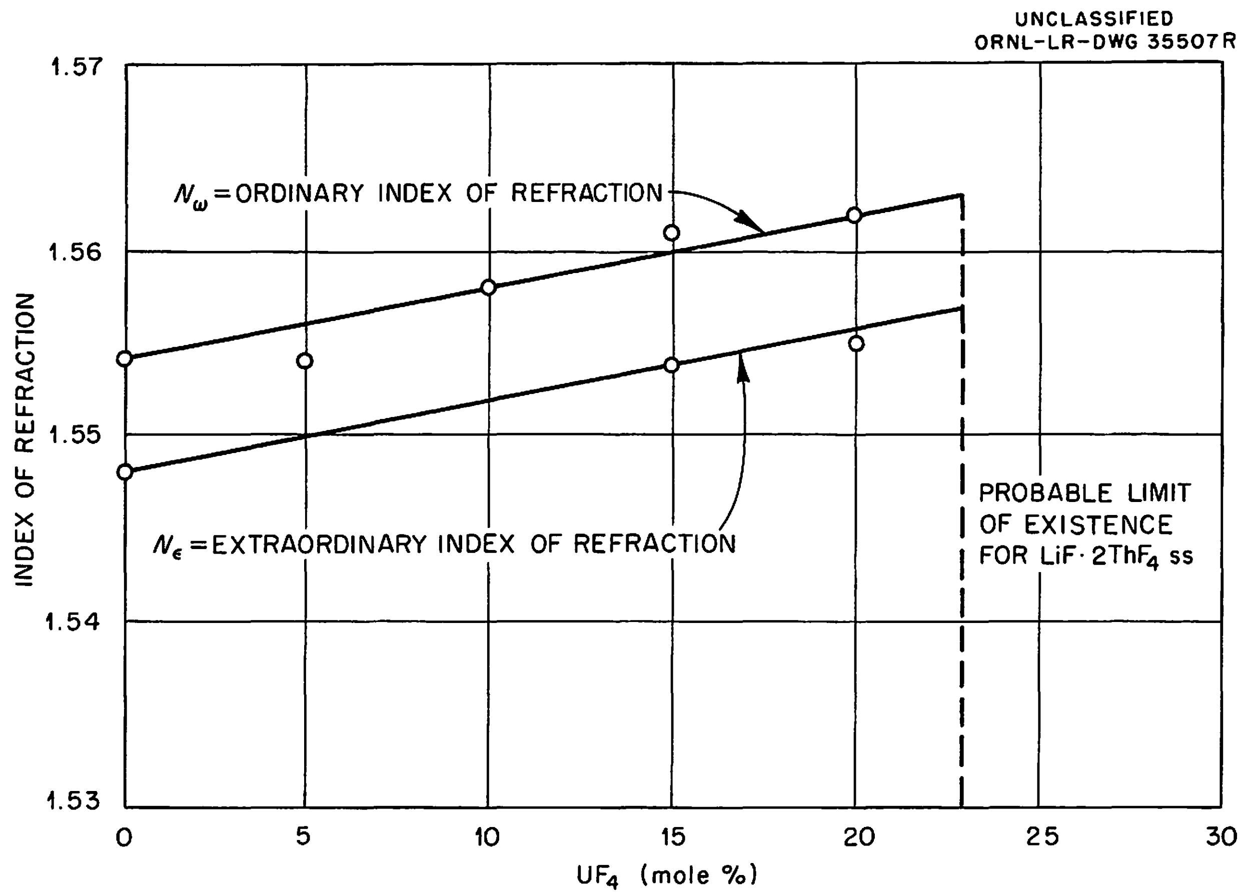

Fig. 11. Indices of Refraction vs Composition for $LiF \cdot 2Th(U)F_4$ (ss).

Table 11. Refractive Index Data for $LiF \cdot 2ThF_4$ (ss)

UF_4 Content (mole %)	Refractive Indices	
	N_ω	N_ϵ
5	1.554	
10	1.558	
15	1.561	1.554
20	1.562	1.555

UNCLASSIFIED
ORNL-LR-DWG 27917AR

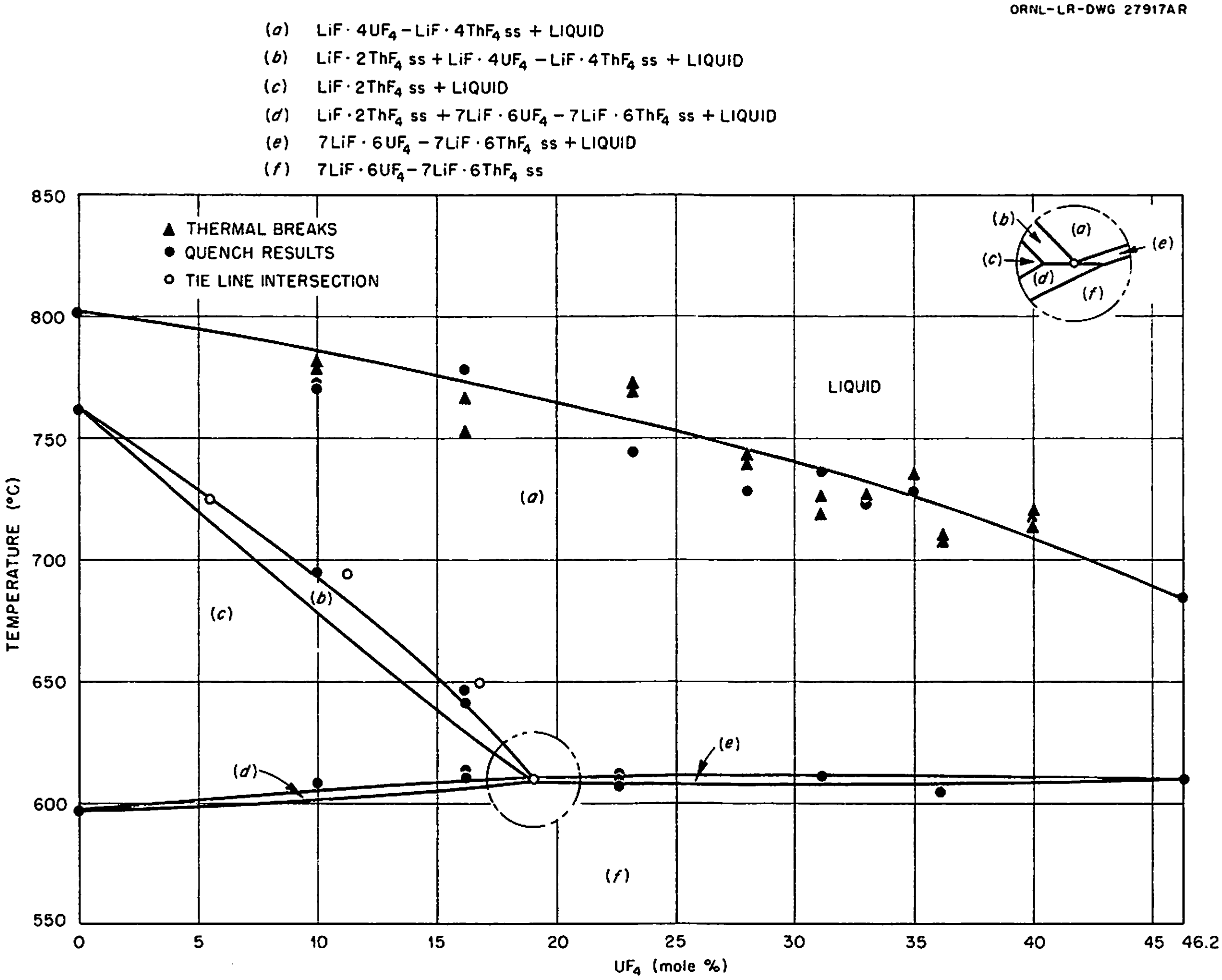

Fig. 12. The Join $7LiF \cdot 6ThF_4$–$7LiF \cdot 6UF_4$.

Table 12. Thermal-Gradient Quenching Data for the 53.8 Mole % LiF Join[a]

UF_4 Content (mole %)	Temperature[b] (°C)	Phases[c] Above Temperature	Phases[c] Below Temperature
10	695 ± 5	Liquid + $LiF{\cdot}4UF_4$–$LiF{\cdot}4ThF_4$ (ss)	Liquid + $LiF{\cdot}2ThF_4$ (ss)
	608 ± 3	Liquid + $LiF{\cdot}2ThF_4$ (ss)	$7LiF{\cdot}6UF_4$–$7LiF{\cdot}6ThF_4$ (ss)
16.2	646 ± 2	Liquid + $LiF{\cdot}4UF_4$–$LiF{\cdot}4ThF_4$ (ss)[d]	Liquid + $LiF{\cdot}2ThF_4$ (ss)[d]
	642 ± 4	Liquid + $LiF{\cdot}4UF_4$–$LiF{\cdot}4ThF_4$ (ss)	Liquid + $LiF{\cdot}2ThF_4$ (ss)
	612 ± 3	Liquid + $LiF{\cdot}2ThF_4$ (ss)	$7LiF{\cdot}6UF_4$–$7LiF{\cdot}6ThF_4$ (ss)[d]
	611 ± 4	Liquid + $LiF{\cdot}2ThF_4$ (ss)	Liquid + $LiF{\cdot}2ThF_4$ (ss) + $7LiF{\cdot}6UF_4$–$7LiF{\cdot}6ThF_4$ (ss)
23.1	612 ± 3	Liquid + $LiF{\cdot}4UF_4$–$LiF{\cdot}4ThF_4$ (ss)	Liquid + $LiF{\cdot}4UF_4$–$LiF{\cdot}4ThF_4$ (ss) + $7LiF{\cdot}6UF_4$–$7LiF{\cdot}6ThF_4$ (ss)
	611 ± 3	Liquid + $LiF{\cdot}4UF_4$–$LiF{\cdot}4ThF_4$ (ss) + $7LiF{\cdot}6UF_4$–$7LiF{\cdot}6ThF_4$ (ss)	$7LiF{\cdot}6UF_4$–$7LiF{\cdot}6ThF_4$ (ss)
	607 ± 2	Liquid + $LiF{\cdot}4UF_4$–$LiF{\cdot}4ThF_4$ (ss) + $7LiF{\cdot}6UF_4$–$7LiF{\cdot}6ThF_4$ (ss)	$7LiF{\cdot}6UF_4$–$7LiF{\cdot}6ThF_4$ (ss)
31.2	611 ± 3	Liquid + $LiF{\cdot}4UF_4$–$LiF{\cdot}4ThF_4$ (ss)	$7LiF{\cdot}6UF_4$–$7LiF{\cdot}6ThF_4$ (ss)
36.2	642 ± 4	Liquid + $LiF{\cdot}4UF_4$–$LiF{\cdot}4ThF_4$ (ss)	Liquid + $LiF{\cdot}2ThF_4$ (ss)

[a]See Table 4 for liquidus values.

[b]The uncertainty in temperatures indicates the temperature differences between the quenched samples.

[c]Only phases found in major quantity are given. Minor quantities of other phases resulting from lack of complete reaction between solids or from trace amounts of oxide impurities are not noted. Glasses or poorly formed crystals assumed to have been produced during rapid cooling of liquid were found in those samples for which the observed phase is indicated as "liquid."

[d]Most of the phases were identified by optical microscopy; this phase was also identified by x-ray diffraction.

Table 13. Tie-Line Data for $7LiF{\cdot}6UF_4$–$7LiF{\cdot}6ThF_4$ (ss) Primary-Phase Area

Quench Composition (mole %)		Temperature Range (°C)	Index of Refraction, N_ω	Solid Solution Composition (mole % UF_4)
UF_4	ThF_4			
2	29	586–591	1.508	5.5
4	27	558–592	1.510	7
5	24	558–563	1.510	7
5	29	557–605	1.512	9
5	31	599	1.512	9
5	33	584–599	1.512	9
5	35	601	1.512	9
6	24	553	1.512	9
7	26	550–607	1.510	7
10	20	546–568	1.516	12.5
10	24	576–593	1.516	12.5
10	26	597	1.515	12
12.5	17	536–562	1.524	19.5
13	30	578–610	1.518	14.5
15	17	585	1.520	16
15	25	532–606	1.519	15
15	28	578–610	1.520	16
16	12	525	1.524	19.5
17	12.5	521–547	1.525	20.5
17	26	578–610	1.522	18
18	18	554–608	1.520	16
18	20	601–612	1.522	18
		554–608	1.522	18
18	22	521	1.524	19.5
		607	1.522	18
		608	1.522	18
18	24	532–612	1.522	18
20	20	520–620	1.526	21.5
20	22	612	1.524	19.5
		532	1.526	21.5
21.5	21.5	596–607	1.526	21.5
25	15	528–609	1.532	26.5
		601	1.534	28.5
		510–612	1.532	26.5
26.5	2	497	1.548	41
27	2	493	1.550	42.5
28	1	497	1.550	42.5
28	10	608	1.534	28.5
		544	1.536	30
30	10	609	1.536	30
		528	1.538	32
33	10	596–601	1.540	34
35	5	528–604	1.544	37.5
		606	1.544	37.5
		510	1.546	39
39	4	553–609	1.547	40

Table 14. Optical Properties for $7LiF \cdot 6UF_4$–$7LiF \cdot 6ThF_4$ (ss)

UF_4 Content (mole %)	Index of Refraction, N_ω	Birefringence
10	1.514	0.003
16.2	1.522	Low
23.1	1.528	Very low
	1.529	Very low
	1.530	Very low
31.2	1.538	Very low
36.2	1.540	Low
	1.542	Low

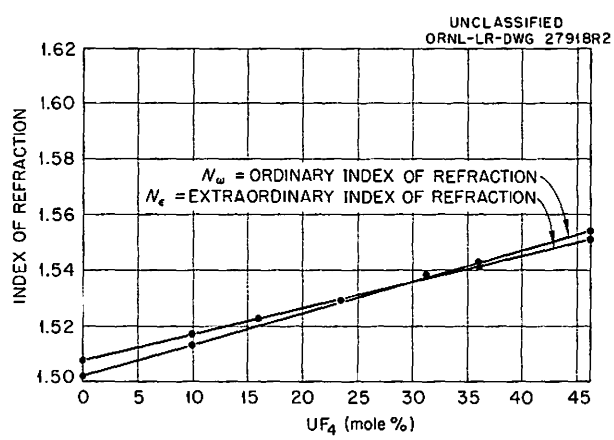

Fig. 13. Indices of Refraction vs Composition for $7LiF \cdot 6ThF_4$–$7LiF \cdot 6UF_4$ (ss).

studies in Tables 4, 15, and 16. The join contains the $3LiF \cdot ThF_4$ (ss) series, whose members are green, biaxial negative, and have optic angles of approximately 10°. The indices of refraction of these solid solutions shown in Fig. 15 and Table 17 vary linearly with UF_4 concentration. The maximum extent of $3LiF \cdot Th(U)F_4$ (ss) is 15.5 mole % UF_4.

The fractionation paths for $3LiF \cdot Th(U)F_4$ (ss) primary-phase area shown in Fig. 7 are based on the tie-line data in Table 16.

RELATIONS BETWEEN THE SOLID SOLUTIONS

Compatibility Triangles

Since the composition of each of the phases in equilibrium at each of the invariant points has been determined, this information can be used to construct the compatibility triangles associated with the invariant points. Figure 16 shows these triangles and is based on the tie-line data in Table 18.

The position of the invariant-point compositions relative to their compatibility triangles indicates that the invariant points at 609, 500, and 488°C are peritectic, peritectic, and eutectic, respectively. These conclusions are in agreement with those in the section "General Discussion of the System LiF-UF_4-ThF_4 and the Limiting Binary Systems," this report.

The direction of decreasing temperature along the boundary line between the primary-phase areas of $7LiF \cdot 6UF_4$–$7LiF \cdot 6ThF_4$ (ss) and $LiF \cdot 4UF_4$–$LiF \cdot 4ThF_4$ (ss) is difficult to determine because the temperature variation along this boundary line is less than 5°C. The relative directions of the tie lines from the 609°C invariant point to the corners of the associated compatibility triangle (Fig. 16) indicate, however, that this boundary temperature decreases in the direction of the ternary invariant composition.

Subsolidus Two-Phase Regions

For a point representing a specified composition in any two-phase subsolidus region in the system LiF-UF_4-ThF_4, the tie line connecting the compositions of the two phases in equilibrium at that point must be a straight line passing through the point. This fact provides a method for checking the accuracy of the refractive index curves (Figs. 8, 11, 13, and 15) of the ternary solid solutions. Tie-line data are given in Table 19 for the following regions:

$$LiF + 3LiF \cdot Th(U)F_4 \text{ (ss)}$$

$$LiF + 7LiF \cdot 6ThF_4\text{–}7LiF \cdot 6UF_4 \text{ (ss)}$$

$$3LiF \cdot Th(U)F_4 \text{ (ss)} + 7LiF \cdot 6ThF_4\text{–}7LiF \cdot 6UF_4 \text{ (ss)}$$

The ends of these tie lines and the corresponding points of nominal composition are shown (Fig. 17) to be nearly colinear.

UNCLASSIFIED
ORNL-LR-DWG 35503R

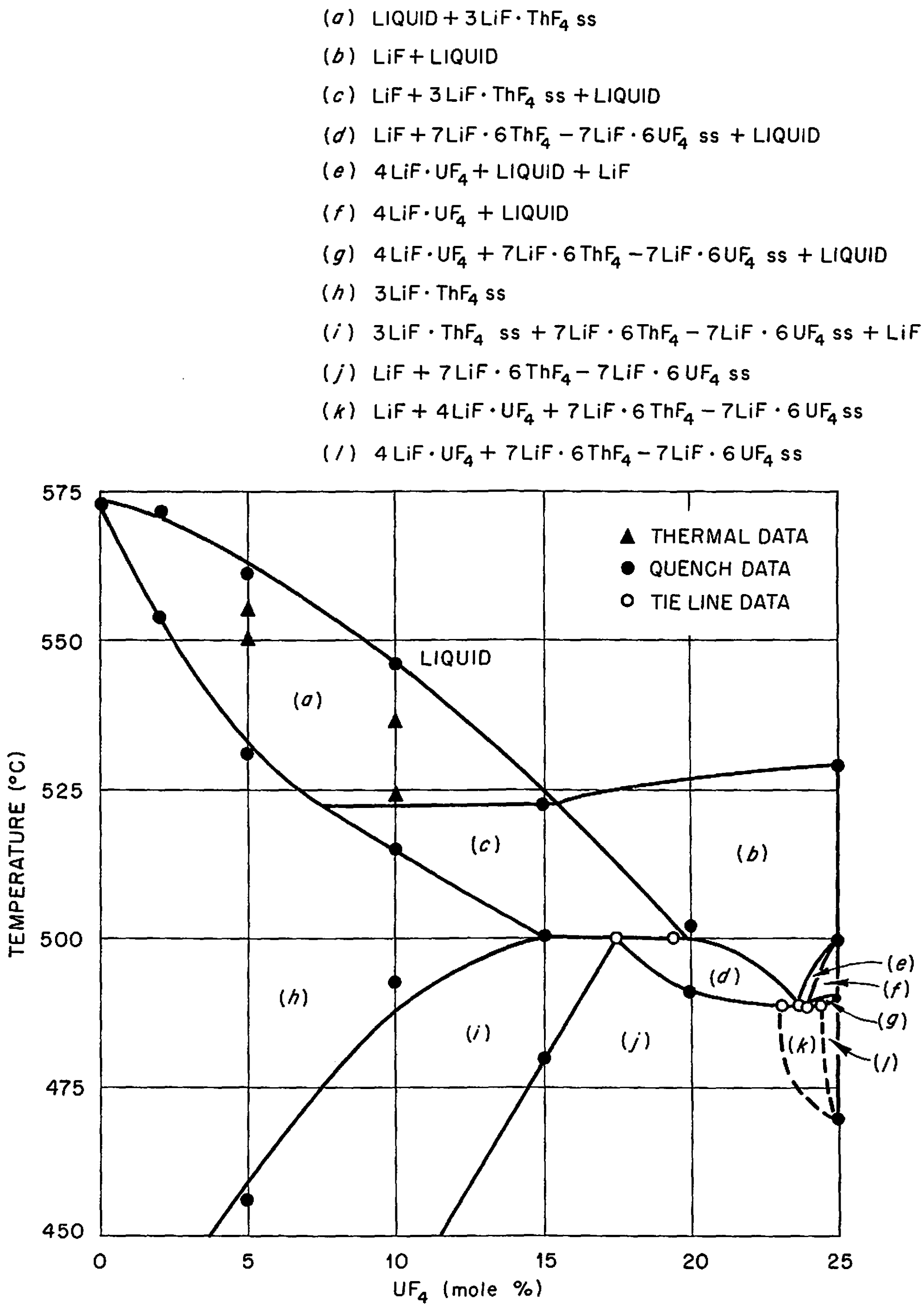

Fig. 14. The 75 Mole % LiF Section.

Table 15. Thermal-Gradient Quenching Data for the 75 Mole % LiF Join[a]

UF_4 Content (mole %)	Temperature[b] (°C)	Phases[c] Above Temperature	Phases[c] Below Temperature
2	554 ± 4	Liquid + $3LiF \cdot ThF_4$ (ss)	$3LiF \cdot ThF_4$ (ss)
5	533 ± 3	Liquid + $3LiF \cdot ThF_4$ (ss)	$3LiF \cdot ThF_4$ (ss)
	460 ± 2[d]	$3LiF \cdot ThF_4$ (ss)[e]	$3LiF \cdot ThF_4$[e] + $7LiF \cdot 6UF_4$–$7LiF \cdot 6ThF_4$ (ss)[e]
10	515 ± 10	Liquid + $3LiF \cdot ThF_4$ (ss)	$3LiF \cdot ThF_4$ (ss)
	493 ± 5	$3LiF \cdot ThF_4$ (ss)[e]	$3LiF \cdot ThF_4$ (ss)[e] + LiF + $7LiF \cdot 6UF_4$–$7LiF \cdot 6ThF_4$ (ss)
13	506 ± 3	Liquid + $3LiF \cdot ThF_4$ (ss)	$3LiF \cdot ThF_4$ (ss)
	491 ± 3	$3LiF \cdot ThF_4$ (ss)[e]	$3LiF \cdot ThF_4$ (ss)[e] + LiF + $7LiF \cdot 6UF_4$–$7LiF \cdot 6ThF_4$ (ss)[e]
15	500 ± 3	Liquid (traces) + LiF (traces) + $3LiF \cdot 6ThF_4$ (ss)[e]	LiF + $3LiF \cdot ThF_4$ (ss) + $7LiF \cdot 6UF_4$–$7LiF \cdot 6ThF_4$ (ss)
	480 ± 2	LiF + $3LiF \cdot ThF_4$ (ss)[e] + $7LiF \cdot 6UF_4$–$7LiF \cdot 6ThF_4$ (ss)[e]	LiF + $7LiF \cdot 6UF_4$–$7LiF \cdot 6ThF_4$ (ss)[e]
20	503 ± 5	Liquid + LiF	Liquid + LiF + $7LiF \cdot 6UF_4$–$7LiF \cdot 6ThF_4$ (ss)[e]
	491 ± 2	Liquid + LiF + $7LiF \cdot 6UF_4$–$7LiF \cdot 6ThF_4$ (ss)	LiF + $7LiF \cdot 6UF_4$–$7LiF \cdot 6ThF_4$ (ss)[e]

[a]See Table 4 for liquidus values.

[b]The uncertainty in temperatures indicates the temperature differences between the quenched samples.

[c]Only phases found in major quantity are given. Minor quantities of other phases resulting from lack of complete reaction between solids or from trace amounts of oxide impurities are not noted. Glasses or poorly formed crystals assumed to have been produced during rapid cooling of liquid were found in those samples for which the observed phase is indicated as "liquid."

[d]This exsolution was observed by using x-ray diffraction technique only.

[e]Most of the phases were identified by optical microscopy; this phase was also identified by x-ray diffraction.

Table 16. Tie-Line Data for $3LiF \cdot ThF_4$ (ss) Primary-Phase Area

Quench Composition (mole %)		Temperature Range (°C)	Index of Refraction, N_γ	Solid Solution Composition (mole % UF_4)
UF_4	ThF_4			
2	24	559	1.490	2.0
5	19	560	1.490	2
10	16	535	1.496	6.5
12	15	530	1.495	6.0
15	12	514–525	1.500	10.0
16	11	513	1.500	10.0
18	10	504–510	1.500	10.0
20	8	504	1.503	12.5

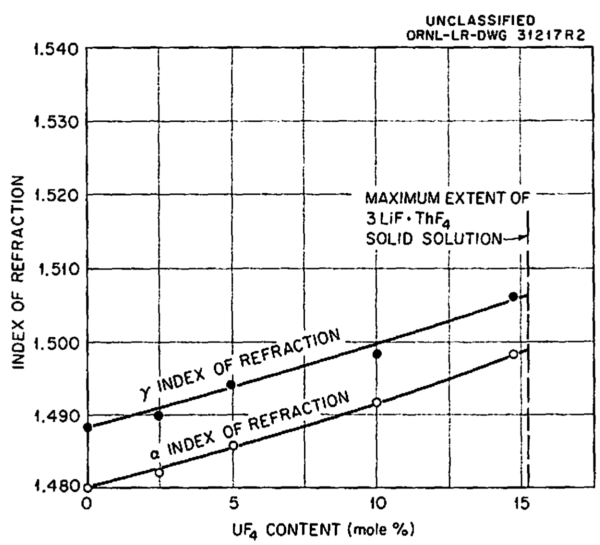

Fig. 15. Indices of Refraction vs Composition for $3LiF \cdot ThF_4$ (ss).

Isothermal Sections

The equilibrium-phase behavior of a ternary system involving solid solutions can be clearly and unambiguously described only by an extensive series of isothermal sections. An abbreviated series of such sections for the system LiF-UF_4-ThF_4 is presented in Figs. 18 through 21. These show the polyphase equilibria for all compositions at the temperatures specified.

Table 17. Refractive Indices for $3LiF \cdot ThF_4$ (ss)

UF_4 Content (mole %)	Refractive Indices	
	N_α	N_γ
2	1.482	1.490
5	1.486	1.494
10	1.492	1.498
13	1.496	1.503
15	1.498	1.507

ACKNOWLEDGMENTS

It is a pleasure to acknowledge the assistance of T. N. McVay, who was responsible for all the refractive index measurements in the system UF_4-ThF_4 and a portion of the petrographic phase identification in the system LiF-UF_4-ThF_4. In addition we are especially grateful to R. F. Newton, F. F. Blankenship, and J. E. Ricci for helpful advice concerning many phases of the investigation.

UNCLASSIFIED
ORNL-LR-DWG 35504

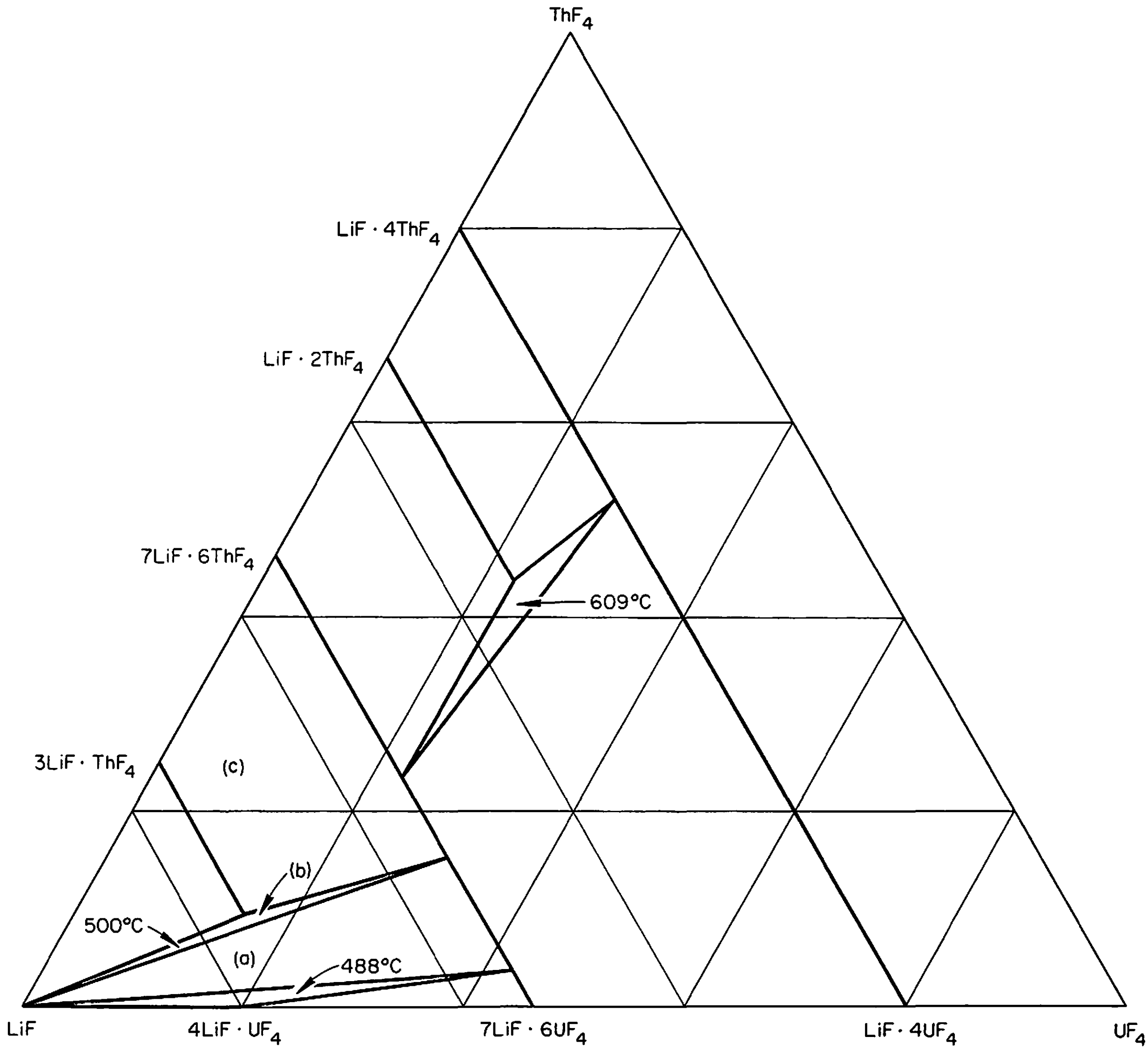

Fig. 16. Compatibility Triangles in the System $LiF\text{-}UF_4\text{-}ThF_4$.

Table 18. Compatibility Triangle Data

Quench Composition (mole %)		Phases Present*	Refractive Indices of Solid Solution		Composition of Solid Solution (mole % UF_4)
UF_4	ThF_4		N_ω	N_γ	
27	1	$7LiF \cdot 6UF_4$–$7LiF \cdot 6ThF_4$ (ss)	1.550		42.5
		$4LiF \cdot UF_4$			
		LiF			
28	1	$7LiF \cdot 6UF_4$–$7LiF \cdot 6ThF_4$ (ss)	1.550		42.5
		$4LiF \cdot UF_4$			
		LiF			
26.5	1	$7LiF \cdot 6UF_4$–$7LiF \cdot 6ThF_4$ (ss)	1.550		42.5
		$4LiF \cdot UF_4$			
		LiF			
27	2	$7LiF \cdot 6UF_4$–$7LiF \cdot 6ThF_4$ (ss)	1.550		42.5
		$4LiF \cdot UF_4$			
		LiF			
15	10	$7LiF \cdot 6UF_4$–$7LiF \cdot 6ThF_4$ (ss)**	1.538	1.506	32
		$3LiF \cdot ThF_4$ (ss)**		1.506	15
		LiF			
17	11	$7LiF \cdot 6UF_4$–$7LiF \cdot 6ThF_4$ (ss)	1.536		30
		$3LiF \cdot ThF_4$ (ss)		1.504	13.5
		LiF			
20	8	$7LiF \cdot 6UF_4$–$7LiF \cdot 6ThF_4$ (ss)**	1.537		31
		$3LiF \cdot ThF_4$ (ss)**		1.504	13.5
		LiF			
18	10	$7LiF \cdot 6UF_4$–$7LiF \cdot 6ThF_4$ (ss)	1.536		30
		$3LiF \cdot ThF_4$ (ss)		1.504	13.5
		LiF			
18	22	$LiF \cdot 4UF_4$–$LiF \cdot 4ThF_4$ (ss)		1.558	28
		$LiF \cdot 2ThF_4$ (ss)**	1.564		23
		$7LiF \cdot 6UF_4$–$7LiF \cdot 6ThF_4$ (ss)**	1.524		23

*Only phases found in major quantity are given. Minor quantities of other phases resulting from lack of complete reaction between solids or from trace amounts of oxide impurities are not noted. Glasses or poorly formed crystals assumed to have been produced during rapid cooling of liquid were found in those samples for which the observed phase is indicated as "liquid."

**Most of the phases were identified by optical microscopy; this phase was also identified by x-ray diffraction.

Table 19. Subsolidus Two-Phase Regions

Quench Composition (mole %)		Phases Present*	Refractive Indices of Solid Solution		Composition of Solid Solution (mole % UF_4)
UF_4	ThF_4		N_γ	N_ω	
4	19	LiF			
		$3LiF \cdot ThF_4$ (ss)**	1.493		4
5	15	LiF			
		$3LiF \cdot ThF_4$ (ss)**	1.495		6.5
8	15	LiF			
		$3LiF \cdot ThF_4$ (ss)**	1.498		9
10	10	LiF			
		$7LiF \cdot 6UF_4$–$7LiF \cdot 6ThF_4$ (ss)**		1.528	22
15	10	LiF			
		$7LiF \cdot 6UF_4$–$7LiF \cdot 6ThF_4$ (ss)		1.524	28
20	5	LiF**			
		$7LiF \cdot 6UF_4$–$7LiF \cdot 6ThF_4$ (ss)**		1.542	36
22	6	LiF**			
		$7LiF \cdot 6UF_4$–$7LiF \cdot 6ThF_4$ (ss)**		1.542	35.5
24	4	LiF**			
		$7LiF \cdot 6UF_4$–$7LiF \cdot 6ThF_4$ (ss)**		1.546	39.5
25	3	LiF			
		$7LiF \cdot 6UF_4$–$7LiF \cdot 6ThF_4$ (ss)		1.548	41
26.5	2	LiF			
		$7LiF \cdot 6UF_4$–$7LiF \cdot 6ThF_4$ (ss)		1.548	41
4	27	$3LiF \cdot ThF_4$ (ss)**	1.490		2
		$7LiF \cdot 6UF_4$–$7LiF \cdot 6ThF_4$ (ss)**		1.510	7
5	24	$3LiF \cdot ThF_4$ (ss)	1.492		3
		$7LiF \cdot 6UF_4$–$7LiF \cdot 6ThF_4$ (ss)		1.512	9
5	29	$3LiF \cdot ThF_4$ (ss)	1.490		2
		$7LiF \cdot 6UF_4$–$7LiF \cdot 6ThF_4$ (ss)		1.512	9
10	16	$3LiF \cdot ThF_4$ (ss)	1.498		8
		$7LiF \cdot 6UF_4$–$7LiF \cdot 6ThF_4$ (ss)		1.528	23.5
6	24	$3LiF \cdot ThF_4$ (ss)	1.494		5
		$7LiF \cdot 6UF_4$–$7LiF \cdot 6ThF_4$ (ss)		1.514	10
10	18	$3LiF \cdot ThF_4$ (ss)	1.498		8
		$7LiF \cdot 6UF_4$–$7LiF \cdot 6ThF_4$ (ss)		1.526	21.5
10	20	$3LiF \cdot ThF_4$ (ss)	1.496		6.5
		$7LiF \cdot 6UF_4$–$7LiF \cdot 6ThF_4$ (ss)		1.522	18
12	15	$3LiF \cdot ThF_4$ (ss)	1.500		10
		$7LiF \cdot 6UF_4$–$7LiF \cdot 6ThF_4$ (ss)		1.530	25
12.5	17	$3LiF \cdot ThF_4$ (ss)	1.496		6.5
		$7LiF \cdot 6UF_4$–$7LiF \cdot 6ThF_4$ (ss)		1.528	23.5
17	12.5	$3LiF \cdot ThF_4$ (ss)	1.504		13
		$7LiF \cdot 6UF_4$–$7LiF \cdot 6ThF_4$ (ss)		1.532	26.5

*Only phases found in major quantity are given. Minor quantities of other phases resulting from lack of complete reaction between solids or from trace amounts of oxide impurities are not noted. Glasses or poorly formed crystals assumed to have been produced during rapid cooling of liquid were found in those samples for which the observed phase is indicated as "liquid."

**Most of the phases were identified by optical microscopy; this phase was also identified by x-ray diffraction.

UNCLASSIFIED
ORNL—LR—DWG 35740R

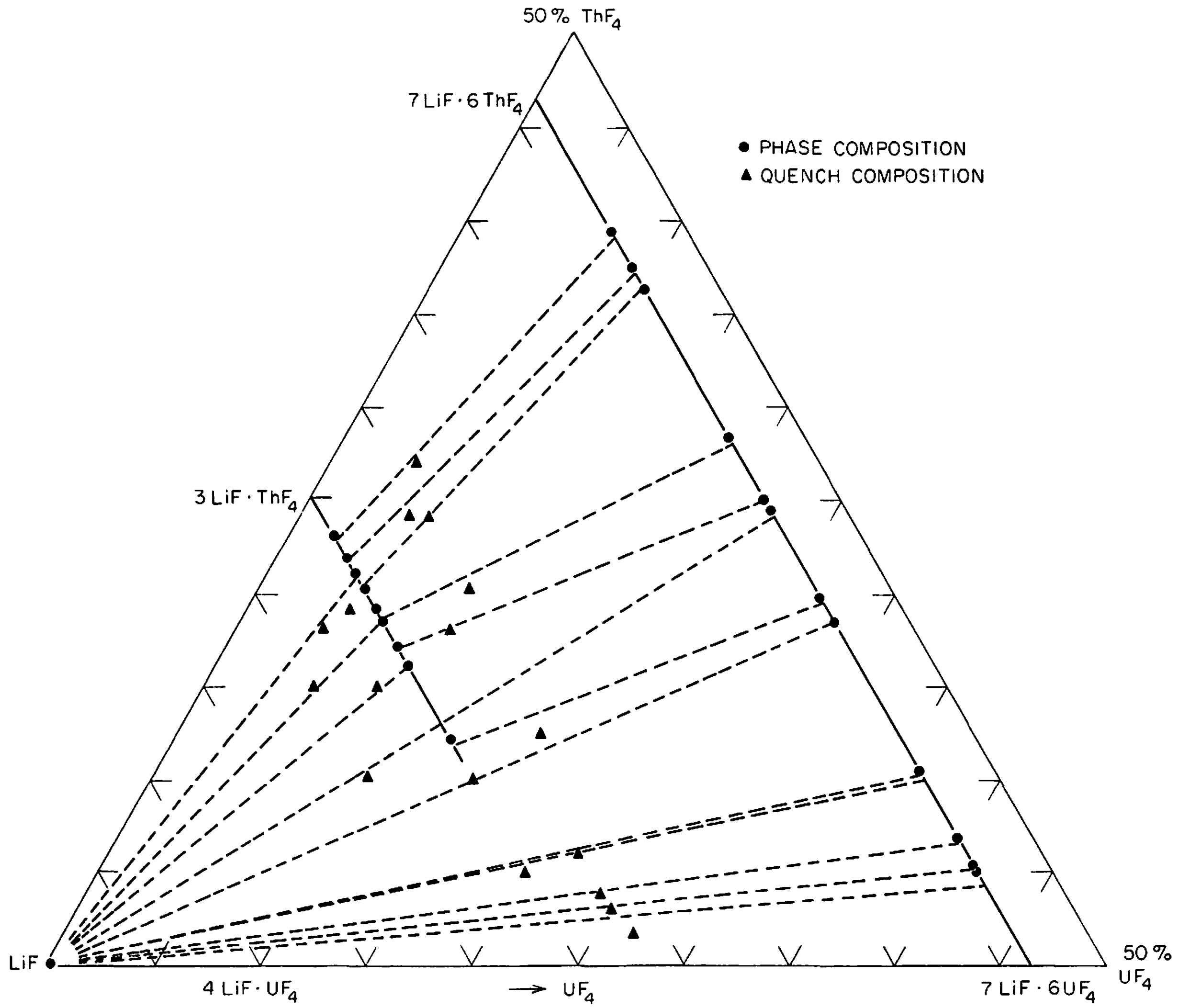

Fig. 17. Subsolidus Tie Lines.

UNCLASSIFIED
ORNL–LR–DWG 35742

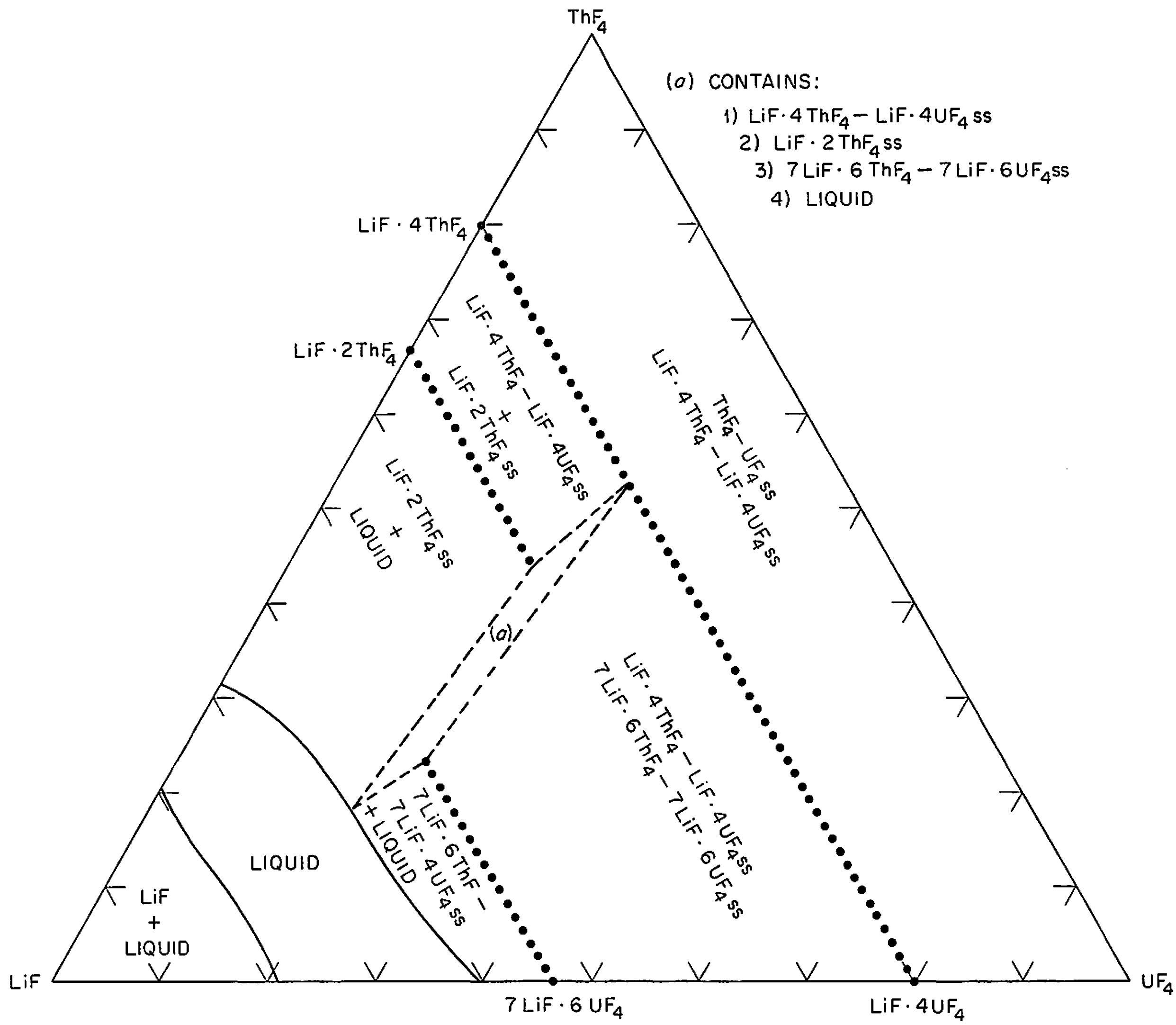

Fig. 18. 609°C Isothermal Section.

UNCLASSIFIED
ORNL—LR—DWG 35741

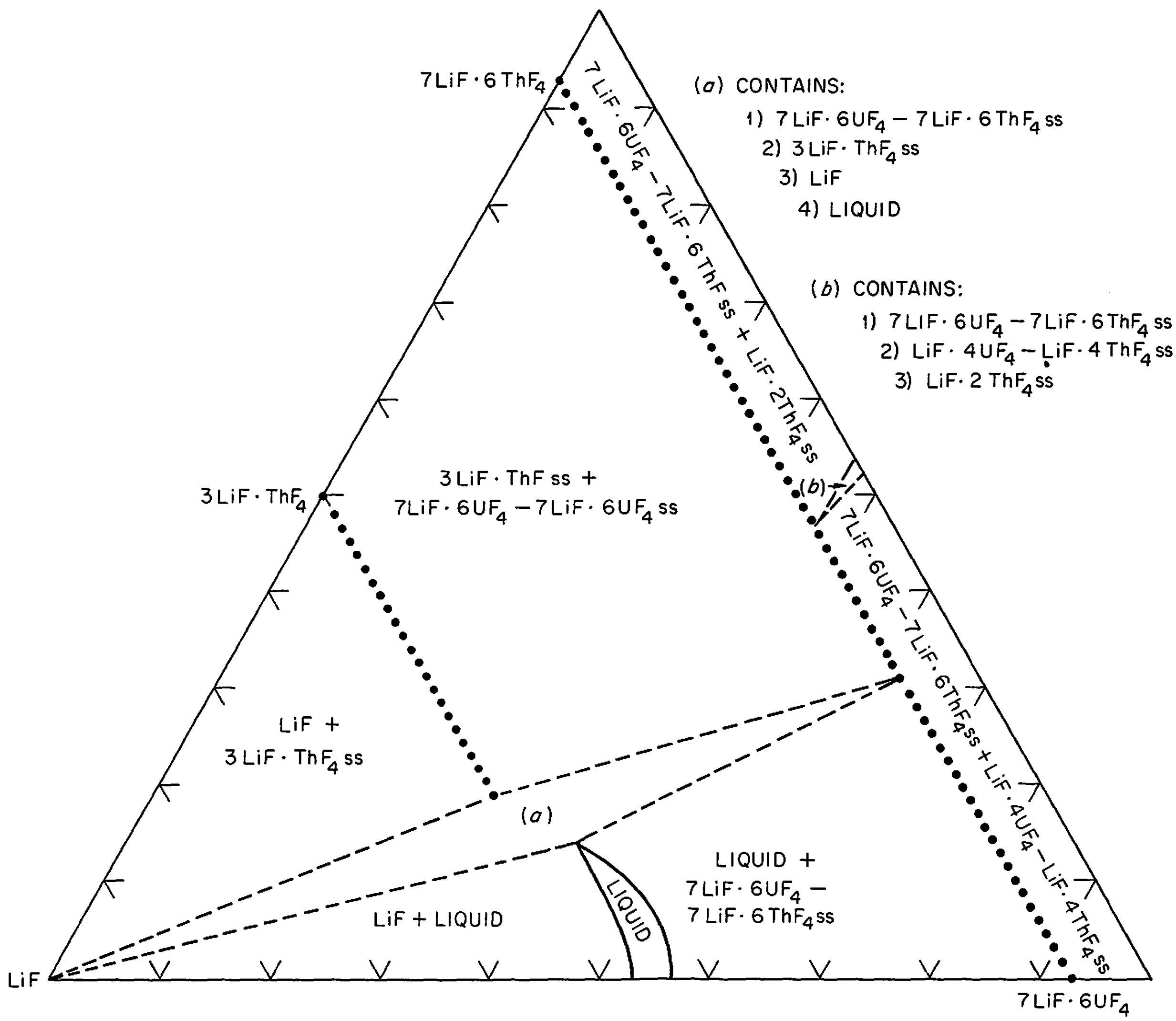

Fig. 19. 500°C Isothermal Section.

UNCLASSIFIED
ORNL—LR—DWG 35738

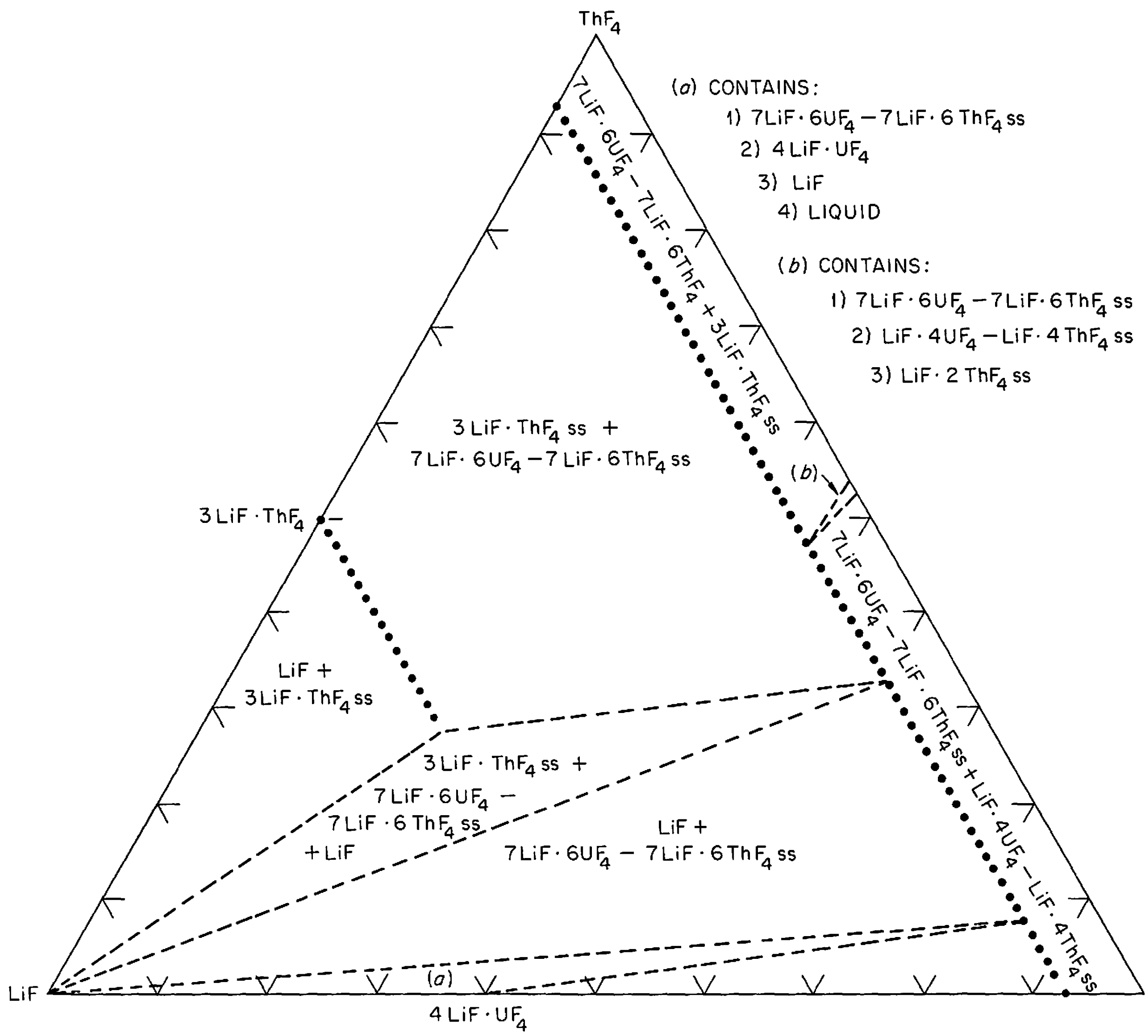

Fig. 20. 488°C Isothermal Section.

UNCLASSIFIED
ORNL—LR—DWG 35739

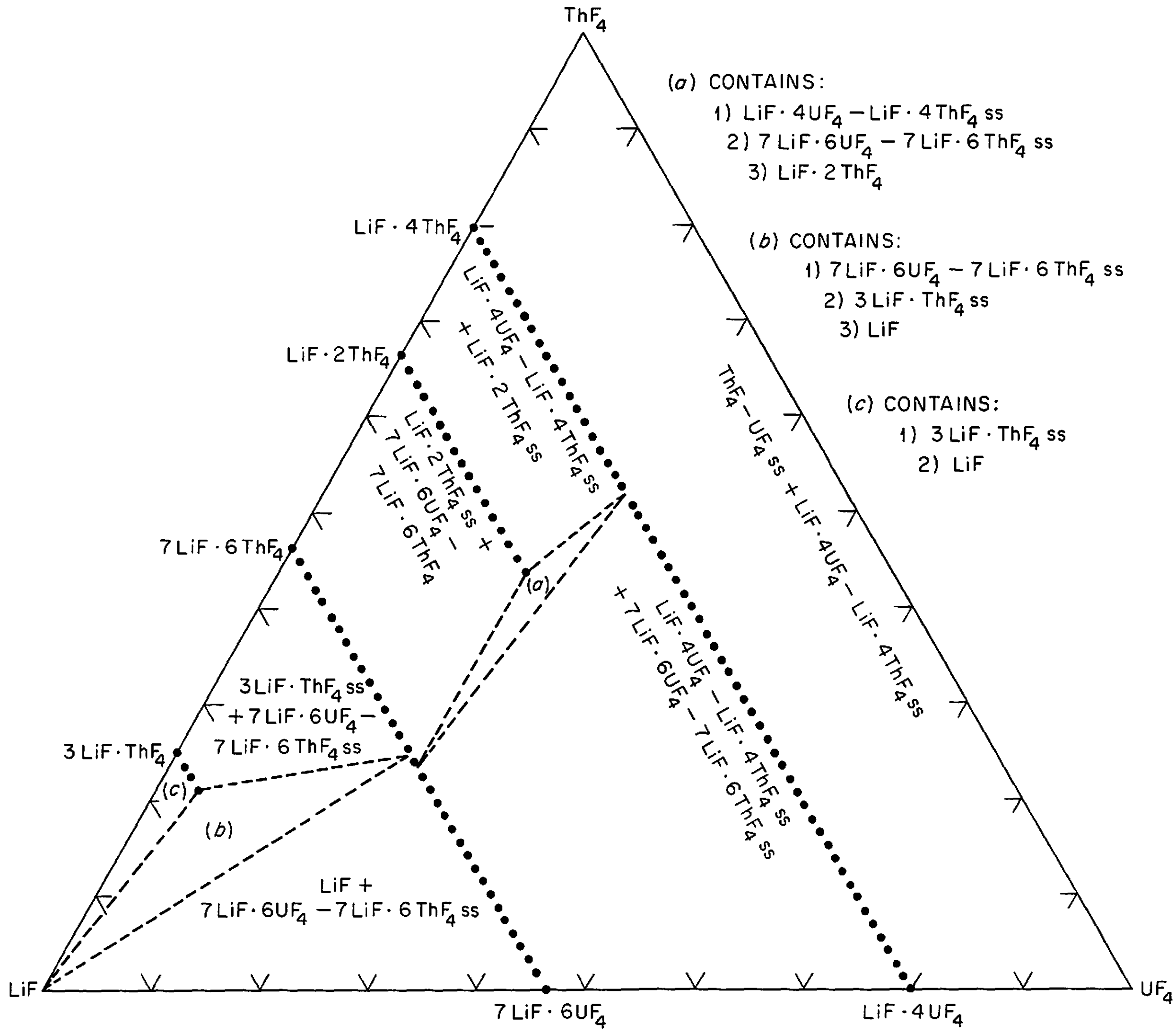

Fig. 21. 450°C Isothermal Section.

Appendix

MISCELLANEOUS THERMAL-GRADIENT QUENCHING RESULTS FOR THE SYSTEM $LiF-UF_4-ThF_4$

Composition (mole %)		Temperature[a] (°C)	Phases[b] Above Temperature	Phases[b] Below Temperature
UF_4	ThF_4			
2	24	522 ± 4	Liquid + $3LiF \cdot ThF_4$ (ss)	Liquid + $3LiF \cdot ThF_4$ (ss) + $7LiF \cdot 6UF_4$–$7LiF \cdot 6ThF_4$ (ss)
2	29	563 ± 3	Liquid + $7LiF \cdot 6UF_4$–$7LiF \cdot 6ThF_4$ (ss)	Liquid + $7LiF \cdot 6UF_4$–$7LiF \cdot 6ThF_4$ (ss) + $3LiF \cdot ThF_4$ (ss)
3	19	561 ± 3	Liquid + LiF	Liquid + LiF + $3LiF \cdot ThF_4$ (ss)
4	19	532 ± 7	Liquid + LiF + $3LiF \cdot ThF_4$ (ss)	LiF + $7LiF \cdot 6UF_4$–$7LiF \cdot 6ThF_4$ (ss)[c]
4	27	555 ± 4	Liquid + $7LiF \cdot 6UF_4$–$7LiF \cdot 6ThF_4$ (ss)	LiF + $3LiF \cdot ThF_4$ (ss) + $7LiF \cdot 6UF_4$–$7LiF \cdot 6ThF_4$ (ss)
		548 ± 4	Liquid + $7LiF \cdot 6UF_4$–$7LiF \cdot 6ThF_4$ (ss) + $3LiF \cdot ThF_4$ (ss)	$7LiF \cdot 6UF_4$–$7LiF \cdot 6ThF_4$ (ss) + $3LiF \cdot ThF_4$ (ss)
5	15	556 ± 4	Liquid + LiF	Liquid + LiF + $3LiF \cdot ThF_4$ (ss)
		540 ± 3	Liquid + LiF + $3LiF \cdot ThF_4$ (ss)	LiF + $3LiF \cdot ThF_4$ (ss)[c]
		462 ± 3	LiF + $3LiF \cdot ThF_4$ (ss)	LiF + $3LiF \cdot ThF_4$ (ss) + $7LiF \cdot 6UF_4$–$7LiF \cdot 6ThF_4$ (ss)
5	19	558 ± 2	Liquid + $3LiF \cdot ThF_4$ (ss)	Liquid + $3LiF \cdot ThF_4$ (ss) + LiF
5	24	555 ± 3	Liquid + $7LiF \cdot 6UF_4$–$7LiF \cdot 6ThF_4$ (ss)	Liquid + $3LiF \cdot ThF_4$ (ss) + $7LiF \cdot 6UF_4$–$7LiF \cdot 6ThF_4$ (ss)
		549 ± 3	Liquid + $3LiF \cdot ThF_4$ (ss) + $7LiF \cdot 6UF_4$–$7LiF \cdot 6ThF_4$ (ss)	$7LiF \cdot 6UF_4$–$7LiF \cdot 6ThF_4$ (ss) + $3LiF \cdot ThF_4$ (ss)
5	26	558 ± 2	Liquid + $7LiF \cdot 6UF_4$–$7LiF \cdot 6ThF_4$ (ss)	Liquid + $3LiF \cdot ThF_4$ (ss) + $7LiF \cdot 6UF_4$–$7LiF \cdot 6ThF_4$ (ss)
		546 ± 2	Liquid + $7LiF \cdot 6UF_4$–$7LiF \cdot 6ThF_4$ (ss) + $3LiF \cdot ThF_4$ (ss)	$7LiF \cdot 6UF_4$–$7LiF \cdot 6ThF_4$ (ss) + $3LiF \cdot ThF_4$ (ss)
5	29	615 ± 3	Liquid + $LiF \cdot 2ThF_4$ (ss)	Liquid + $LiF \cdot 2ThF_4$ (ss) + $7LiF \cdot 6UF_4$–$7LiF \cdot 6ThF_4$ (ss)
		605 ± 3	Liquid + $LiF \cdot 2ThF_4$ (ss) + $7LiF \cdot 6UF_4$–$7LiF \cdot 6ThF_4$ (ss)	Liquid + $7LiF \cdot 6UF_4$–$7LiF \cdot 6ThF_4$ (ss)
		557 ± 3	Liquid + $7LiF \cdot 6UF_4$–$7LiF \cdot 6ThF_4$ (ss)	Liquid + $7LiF \cdot 6UF_4$–$7LiF \cdot 6ThF_4$ (ss) + $3LiF \cdot ThF_4$ (ss)
		547 ± 3	Liquid + $7LiF \cdot 6UF_4$–$7LiF \cdot 6ThF_4$ (ss) + $3LiF \cdot ThF_4$ (ss)	$7LiF \cdot 6UF_4$–$7LiF \cdot 6ThF_4$ (ss) + $3LiF \cdot ThF_4$ (ss)
5	31	609 ± 4	Liquid + $LiF \cdot 2ThF_4$ (ss)	Liquid + $LiF \cdot 2ThF_4$ (ss) + $7LiF \cdot 6UF_4$–$7LiF \cdot 6ThF_4$ (ss)
		602 ± 3	Liquid + $LiF \cdot 2ThF_4$ (ss) + $7LiF \cdot 6UF_4$–$7LiF \cdot 6ThF_4$ (ss)	Liquid + $7LiF \cdot 6UF_4$–$7LiF \cdot 6ThF_4$ (ss)

Appendix (continued)

Composition (mole %)		Temperature[a] (°C)	Phases[b] Above Temperature	Phases[b] Below Temperature
UF_4	ThF_4			
5	33	605 ± 3	Liquid + $LiF \cdot 2ThF_4$ (ss)	Liquid + $LiF \cdot 2ThF_4$ (ss) + $7LiF \cdot 6UF_4$–$7LiF \cdot 6ThF_4$ (ss)
		599 ± 3	Liquid + $LiF \cdot 2ThF_4$ (ss) + $7LiF \cdot 6UF_4$–$7LiF \cdot 6ThF_4$ (ss)	Liquid + $7LiF \cdot 6UF_4$–$7LiF \cdot 6ThF_4$ (ss)
5	35	605 ± 4	Liquid + $LiF \cdot 2ThF_4$ (ss)	Liquid + $7LiF \cdot 6UF_4$–$7LiF \cdot 6ThF_4$ (ss)
6	24	551 ± 3	Liquid + $7LiF \cdot 6UF_4$–$7LiF \cdot 6ThF_4$ (ss)	Liquid + $3LiF \cdot ThF_4$ (ss) + $7LiF \cdot 6UF_4$–$7LiF \cdot 6ThF_4$ (ss)
		541 ± 3	Liquid + $3LiF \cdot ThF_4$ (ss) + $7LiF \cdot 6UF_4$–$7LiF \cdot 6ThF_4$ (ss)	$3LiF \cdot ThF_4$ (ss) + $7LiF \cdot 6UF_4$–$7LiF \cdot 6ThF_4$ (ss)
7	26	547 ± 3	Liquid + $7LiF \cdot 6UF_4$–$7LiF \cdot 6ThF_4$ (ss)	Liquid + $3LiF \cdot ThF_4$ (ss) + $7LiF \cdot 6UF_4$–$7LiF \cdot 6ThF_4$ (ss)
8	15	517 ± 3	Liquid + LiF + $3LiF \cdot ThF_4$ (ss)	LiF + $3LiF \cdot ThF_4$ (ss)
		480 ± 2	LiF + $3LiF \cdot ThF_4$ (ss)[c]	LiF + $3LiF \cdot ThF_4$ (ss) + $7LiF \cdot 6UF_4$–$7LiF \cdot 6ThF_4$ (ss)
10	10	528 ± 3	LiF + liquid	Liquid + LiF + $3LiF \cdot ThF_4$ (ss)
		488 ± 3	Liquid + LiF + $3LiF \cdot ThF_4$ (ss)	$7LiF \cdot 6UF_4$–$7LiF \cdot 6ThF_4$ (ss)[c] + LiF[c] + $3LiF \cdot ThF_4$ (ss)[c]
		464 ± 3	LiF[c] + $3LiF \cdot ThF_4$ (ss) + $7LiF \cdot 6UF_4$–$7LiF \cdot 6ThF_4$ (ss)[c]	LiF[c] + $7LiF \cdot 6UF_4$–$7LiF \cdot 6ThF_4$ (ss)[c]
10	16	533 ± 2	Liquid + $3LiF \cdot ThF_4$ (ss)	Liquid + $3LiF \cdot ThF_4$ (ss) + $7LiF \cdot 6UF_4$–$7LiF \cdot 6ThF_4$ (ss)
10	18	513 ± 2	Liquid + $3LiF \cdot ThF_4$ (ss) + $7LiF \cdot 6UF_4$–$7LiF \cdot 6ThF_4$ (ss)	$7LiF \cdot 6UF_4$–$7LiF \cdot 6ThF_4$ (ss) + $3LiF \cdot ThF_4$ (ss)
10	20	543 ± 3	Liquid + $7LiF \cdot 6UF_4$–$7LiF \cdot 6ThF_4$ (ss)	Liquid + $3LiF \cdot ThF_4$ (ss) + $7LiF \cdot 6UF_4$–$7LiF \cdot 6ThF_4$ (ss)
		538 ± 2	Liquid + $7LiF \cdot 6UF_4$–$7LiF \cdot 6ThF_4$ (ss) + $3LiF \cdot ThF_4$ (ss)	$7LiF \cdot 6UF_4$–$7LiF \cdot 6ThF_4$ (ss) + $3LiF \cdot ThF_4$ (ss)
10	70	889 ± 4	Liquid + UF_4–ThF_4 (ss)	$LiF \cdot 4UF_4$–$LiF \cdot 4ThF_4$ (ss)
11	32	612 ± 3	Liquid + $LiF \cdot 2ThF_4$ (ss)[c]	Liquid + $LiF \cdot 2ThF_4$ (ss)[c] + $7LiF \cdot 6UF_4$–$7LiF \cdot 6ThF_4$ (ss)[c]
		607 ± 3	Liquid + $LiF \cdot 2ThF_4$ (ss) + $7LiF \cdot 6UF_4$–$7LiF \cdot 6ThF_4$ (ss)	Liquid + $7LiF \cdot 6UF_4$–$7LiF \cdot 6ThF_4$ (ss)
12	15	525 ± 2	Liquid + $3LiF \cdot ThF_4$ (ss)	Liquid + $3LiF \cdot ThF_4$ (ss) + $7LiF \cdot 6UF_4$–$7LiF \cdot 6ThF_4$ (ss)
		505 ± 2	Liquid + $7LiF \cdot 6UF_4$–$7LiF \cdot 6ThF_4$ (ss) + $3LiF \cdot ThF_4$ (ss)	$7LiF \cdot 6UF_4$–$7LiF \cdot 6ThF_4$ (ss) + $3LiF \cdot ThF_4$ (ss)
12.5	17	532 ± 4	Liquid + $7LiF \cdot 6UF_4$–$7LiF \cdot 6ThF_4$ (ss)	Liquid + $3LiF \cdot ThF_4$ (ss) + $7LiF \cdot 6UF_4$–$7LiF \cdot 6ThF_4$ (ss)

Composition (mole %) UF$_4$	ThF$_4$	Temperature[a] (°C)	Phases[b] Above Temperature	Phases[b] Below Temperature
12.5	17	514 ± 3	Liquid + $7LiF \cdot 6UF_4$–$7LiF \cdot 6ThF_4$ (ss) + $3LiF \cdot ThF_4$ (ss)	$7LiF \cdot 6UF_4$–$7LiF \cdot 6ThF_4$ (ss) + $3LiF \cdot ThF_4$ (ss)
13	30	688 ± 2	Liquid + $LiF \cdot 4UF_4$–$LiF \cdot 4ThF_4$ (ss)[c]	Liquid + $LiF \cdot 2ThF_4$ (ss)[c]
		612 ± 3	Liquid + $LiF \cdot 2ThF_4$ (ss)[c]	Liquid + $7LiF \cdot 6UF_4$–$7LiF \cdot 6ThF_4$ (ss)[c]
15	12	511 ± 3	Liquid + $3LiF \cdot ThF_4$ (ss)	Liquid + $3LiF \cdot ThF_4$ (ss) + $7LiF \cdot 6UF_4$–$7LiF \cdot 6ThF_4$ (ss)
15	25	612 ± 4	Liquid + $LiF \cdot 2ThF_4$ (ss)	Liquid + $7LiF \cdot 6UF_4$–$7LiF \cdot 6ThF_4$ (ss)
		529 ± 4	Liquid + $7LiF \cdot 6UF_4$–$7LiF \cdot 6ThF_4$ (ss)	Liquid + $3LiF \cdot ThF_4$ (ss) + $7LiF \cdot 6UF_4$–$7LiF \cdot 6ThF_4$ (ss)
15	28	680 ± 3	Liquid + $LiF \cdot 4UF_4$–$LiF \cdot 4ThF_4$ (ss)	Liquid + $LiF \cdot 2ThF_4$ (ss)
		617 ± 3	Liquid + $LiF \cdot 2ThF_4$ (ss)	Liquid + $LiF \cdot 2ThF_4$ (ss) + $7LiF \cdot 6UF_4$–$7LiF \cdot 6ThF_4$ (ss)
		612 ± 3	Liquid + $LiF \cdot 2ThF_4$ (ss) + $7LiF \cdot 6UF_4$–$7LiF \cdot 6ThF_4$ (ss)	Liquid + $7LiF \cdot 6UF_4$–$7LiF \cdot 6ThF_4$ (ss)[c]
16	11	510 ± 2	Liquid + $3LiF \cdot ThF_4$ (ss)	Liquid + $3LiF \cdot ThF_4$ (ss) + $7LiF \cdot 6UF_4$–$7LiF \cdot 6ThF_4$ (ss)
		501 ± 8	Liquid + $3LiF.ThF_4$ (ss) + $7LiF \cdot 6UF_4$–$7LiF \cdot 6ThF_4$ (ss)	Liquid + $3LiF \cdot ThF_4$ (ss) + $7LiF \cdot 6UF_4$–$7LiF \cdot 6ThF_4$ (ss) + LiF
		492 ± 2	Liquid + $3LiF \cdot ThF_4$ (ss) + $7LiF \cdot 6UF_4$–$7LiF \cdot 6ThF_4$ (ss) + LiF	$3LiF \cdot ThF_4$ (ss) + $7LiF \cdot 6UF_4$–$7LiF \cdot 6ThF_4$ (ss) + LiF
16	12	523 ± 2	Liquid + $7LiF \cdot 6UF_4$–$7LiF \cdot 6ThF_4$ (ss)	Liquid + $3LiF \cdot ThF_4$ (ss) + $7LiF \cdot 6UF_4$–$7LiF \cdot 6ThF_4$ (ss)
17	11	499 ± 5	Liquid + $7LiF \cdot 6UF_4$–$7LiF \cdot 6ThF_4$ (ss) + $3LiF \cdot ThF_4$ (ss)	LiF + $3LiF \cdot ThF_4$ (ss) + $7LiF \cdot 6UF_4$–$7LiF \cdot 6ThF_4$ (ss)
17	12.5	519 ± 3	Liquid + $7LiF \cdot 6UF_4$–$7LiF \cdot 6ThF_4$ (ss)	Liquid + $3LiF \cdot ThF_4$ (ss) + $7LiF \cdot 6UF_4$–$7LiF \cdot 6ThF_4$ (ss)
		507 ± 3	Liquid + $7LiF \cdot 6UF_4$–$7LiF \cdot 6ThF_4$ (ss) + $3LiF \cdot ThF_4$ (ss)	$7LiF \cdot 6UF_4$–$7LiF \cdot 6ThF_4$ (ss) + $3LiF \cdot ThF_4$ (ss)
		490 ± 3	$7LiF \cdot 6UF_4$–$7LiF \cdot 6ThF_4$ (ss) + $3LiF \cdot ThF_4$ (ss)	$3LiF \cdot ThF_4$ (ss) + $7LiF \cdot 6UF_4$–$7LiF \cdot 6ThF_4$ (ss) + LiF
17	26	660 ± 3	Liquid + $LiF \cdot 4UF_4$–$LiF \cdot 4ThF_4$ (ss)	Liquid + $LiF \cdot 2ThF_4$ (ss)[c]
		617 ± 3	Liquid + $LiF \cdot 2ThF_4$ (ss)[c]	Liquid + $LiF \cdot 2ThF_4$ (ss)[c] + $7LiF \cdot 6UF_4$–$7LiF \cdot 6ThF_4$ (ss)[c]
		612 ± 4	Liquid + $LiF \cdot 2ThF_4$ (ss)[c] + $7LiF \cdot 6UF_4$–$7LiF \cdot 6ThF_4$ (ss)[c]	Liquid + $7LiF \cdot 6UF_4$–$7LiF \cdot 6ThF_4$ (ss)
18	10	502 ± 2	Liquid + $3LiF \cdot ThF_4$ (ss)	Liquid + $3LiF \cdot ThF_4$ (ss) + $7LiF \cdot 6UF_4$–$7LiF \cdot 6ThF_4$ (ss)[c]

Appendix (continued)

Composition (mole %)		Temperature[a] (°C)	Phases[b] Above Temperature	Phases[b] Below Temperature
UF_4	ThF_4			
18	10	489 ± 2	Liquid + $3LiF \cdot ThF_4$ (ss) + $7LiF \cdot 6UF_4$–$7LiF \cdot 6ThF_4$ (ss)	$7LiF \cdot 6UF_4$–$7LiF \cdot 6ThF_4$ (ss) + $3LiF \cdot ThF_4$ (ss) + LiF
18	20	637 ± 3	Liquid + $LiF \cdot 4UF_4$–$LiF \cdot 4ThF_4$ (ss)[c]	Liquid + $LiF \cdot 2ThF_4$ (ss)
		615 ± 4	Liquid + $LiF \cdot 2ThF_4$ (ss)[c]	Liquid + $7LiF \cdot 6UF_4$–$7LiF \cdot 6ThF_4$ (ss)
		612 ± 4	Liquid + $LiF \cdot 2ThF_4$ (ss)	Liquid + $7LiF \cdot 6UF_4$–$7LiF \cdot 6ThF_4$ (ss)
18	22	634 ± 4	Liquid + $LiF \cdot 4UF_4$–$LiF \cdot 4ThF_4$ (ss)	Liquid + $LiF \cdot 2ThF_4$ (ss)
		626 ± 3	Liquid + $LiF \cdot 4UF_4$–$LiF \cdot 4ThF_4$ (ss)	Liquid + $LiF \cdot 2ThF_4$ (ss)[c]
		612 ± 3	Liquid + $LiF \cdot 2ThF_4$ (ss)[c]	Liquid + $7LiF \cdot 6UF_4$–$7LiF \cdot 6ThF_4$ (ss)[c]
		612 ± 4	Liquid + $LiF \cdot 2ThF_4$ (ss)[c]	Liquid + $7LiF \cdot 6UF_4$–$7LiF \cdot 6ThF_4$ (ss)[c]
20	8	502 ± 2	Liquid + $3LiF \cdot ThF_4$ (ss)	Liquid + $3LiF \cdot ThF_4$ (ss) + $7LiF \cdot 6UF_4$–$7LiF \cdot 6ThF_4$ (ss)
		498 ± 2	Liquid + $3LiF \cdot ThF_4$ (ss) + $7LiF \cdot 6UF_4$–$7LiF \cdot 6ThF_4$ (ss)	LiF + $3LiF \cdot ThF_4$ (ss) + $7LiF \cdot 6UF_4$–$7LiF \cdot 6ThF_4$ (ss)
20	20	620 ± 3	Liquid + $LiF \cdot 4UF_4$–$LiF \cdot 4ThF_4$ (ss)	Liquid + $7LiF \cdot 6UF_4$–$7LiF \cdot 6ThF_4$ (ss)[c]
		517 ± 2	Liquid + $7LiF \cdot 6UF_4$–$7LiF \cdot 6ThF_4$ (ss)	Liquid + $3LiF \cdot ThF_4$ (ss) + $7LiF \cdot 6UF_4$–$7LiF \cdot 6ThF_4$ (ss)
20	45	883 ± 2	Liquid + UF_4-ThF_4 (ss)	Liquid + $LiF \cdot 4UF_4$–$LiF \cdot 4ThF_4$ (ss)
21.5	21.5	610 ± 3	Liquid + $LiF \cdot 4UF_4$–$LiF \cdot 4ThF_4$ (ss)	Liquid + $7LiF \cdot 6UF_4$–$7LiF \cdot 6ThF_4$ (ss)[c]
22	6	495 ± 2	LiF + liquid	LiF + liquid + $7LiF \cdot 6UF_4$–$7LiF \cdot 6ThF_4$ (ss)
		487 ± 2	LiF + liquid + $7LiF \cdot 6UF_4$–$7LiF \cdot 6ThF_4$ (ss)[c]	$7LiF \cdot 6UF_4$–$7LiF \cdot 6ThF_4$ (ss)[c] + LiF[c]
24	4	488 ± 2	$7LiF \cdot 6UF_4$–$7LiF \cdot 6ThF_4$ (ss) + LiF + liquid	LiF + $7LiF \cdot 6UF_4$–$7LiF \cdot 6ThF_4$ (ss)
25	2	487 ± 2	Liquid + LiF + $7LiF \cdot 6UF_4$–$7LiF \cdot 6ThF_4$ (ss)	LiF + $7LiF \cdot 6UF_4$–$7LiF \cdot 6ThF_4$ (ss)
25	3	491 ± 3	Liquid + LiF + $7LiF \cdot 6UF_4$–$7LiF \cdot 6ThF_4$ (ss)	LiF + $7LiF \cdot 6UF_4$–$7LiF \cdot 6ThF_4$ (ss)
25	15	615 ± 3	Liquid + $LiF \cdot 4UF_4$–$LiF \cdot 4ThF_4$ (ss)	Liquid + $7LiF \cdot 6UF_4$–$7LiF \cdot 6ThF_4$ (ss)
		613 ± 2	Liquid + $LiF \cdot 4UF_4$–$LiF \cdot 4ThF_4$ (ss)	Liquid + $7LiF \cdot 6UF_4$–$7LiF \cdot 6ThF_4$ (ss)
		607 ± 6	Liquid + $LiF \cdot 4UF_4$–$LiF \cdot 4ThF_4$ (ss)	Liquid + $7LiF \cdot 6UF_4$–$7LiF \cdot 6ThF_4$ (ss)
26	2	489 ± 2	Liquid + LiF + $7LiF \cdot 6UF_4$–$7LiF \cdot 6ThF_4$ (ss)[c]	LiF + $7LiF \cdot 6UF_4$–$7LiF \cdot 6ThF_4$ (ss)[c]
26.5	2	495 ± 2	Liquid + $7LiF \cdot 6UF_4$–$7LiF \cdot 6ThF_4$ (ss)	Liquid + LiF + $7LiF \cdot 6UF_4$–$7LiF \cdot 6ThF_4$ (ss)
		490 ± 3	Liquid + LiF + $7LiF \cdot 6UF_4$–$7LiF \cdot 6ThF_4$ (ss)	LiF + $7LiF \cdot 6UF_4$–$7LiF \cdot 6ThF_4$ (ss)

Composition (mole %)		Temperature[a] (°C)	Phases[b] Above Temperature	Phases[b] Below Temperature
UF_4	ThF_4			
28	10	610 ± 3	Liquid + $LiF \cdot 4UF_4$–$LiF \cdot 4ThF_4$ (ss)	Liquid + $7LiF \cdot 6UF_4$–$7LiF \cdot 6ThF_4$ (ss)
30	10	611 ± 2	Liquid + $LiF \cdot 4UF_4$–$LiF \cdot 4ThF_4$ (ss)	Liquid + $7LiF \cdot 6UF_4$–$7LiF \cdot 6ThF_4$ (ss)
30	50	827 ± 5	Liquid + UF_4-ThF_4 (ss)	Liquid + UF_4-ThF_4 (ss) + $LiF \cdot 4UF_4$–$LiF \cdot 4ThF_4$ (ss)
33	10	604 ± 3	Liquid + $LiF \cdot 4UF_4$–$LiF \cdot 4ThF_4$ (ss)	Liquid + $7LiF \cdot 6UF_4$–$7LiF \cdot 6ThF_4$ (ss)
33⅓	33⅓	862 ± 2	Liquid + UF_4-ThF_4 (ss)	Liquid + $LiF \cdot 4UF_4$–$LiF \cdot 4ThF_4$ (ss)
39	4	612 ± 3	Liquid + $LiF \cdot 4UF_4$–$LiF \cdot 4ThF_4$ (ss)	Liquid + $7LiF \cdot 6UF_4$–$7LiF \cdot 6ThF_4$ (ss)
45	20	859 ± 3	Liquid + UF_4-ThF_4 (ss)	Liquid + $LiF \cdot 4UF_4$–$LiF \cdot 4ThF_4$ (ss)

[a] The uncertainty in temperatures indicates the temperature differences between the quenched samples.

[b] Only phases found in major quantity are given. Minor quantities of other phases resulting from lack of complete reaction between solids or from trace amounts of oxide impurities are not noted. Glasses or poorly formed crystals assumed to have been produced during rapid cooling of liquid were found in those samples for which the observed phase is indicated as "liquid."

[c] Most of the phases were identified by optical microscopy; in addition, this phase was identified by x-ray diffraction.

INTERNAL DISTRIBUTION

1. C. E. Center
2. Biology Library
3. Health Physics Library
4–5. Central Research Library
6. Reactor Experimental Engineering Library
7–26. Laboratory Records Department
27. Laboratory Records, ORNL, R.C.
28. A. M. Weinberg
29. L. B. Emlet (K-25)
30. J. P. Murray
31. J. A. Swartout
32. E. H. Taylor
33. E. D. Shipley
34. S. C. Lind
35. M. L. Nelson
36. C. P. Keim
37. J. H. Frye, Jr.
38. R. S. Livingston
39. H. G. MacPherson
40. F. L. Culler
41. A. H. Snell
42. A. Hollaender
43. M. T. Kelley
44. K. Z. Morgan
45. C. F. Weaver
46. A. S. Householder
47. C. S. Harrill
48. C. E. Winters
49. H. E. Seagren
50. D. Phillips
51. F. C. VonderLage
52. D. S. Billington
53. J. A. Lane
54. M. J. Skinner
55. W. H. Jordan
56. G. E. Boyd
57. C. J. Barton
58. J. P. Blakely
59. M. Blander
60. F. F. Blankenship
61. C. M. Blood
62. S. Cantor
63. R. B. Evans
64. H. A. Friedman
65. R. A. Gilbert
66. W. R. Grimes
67. H. Insley
68. F. Kertesz
69. S. Langer
70. R. E. Meadows
71. R. E. Moore
72. G. J. Nessle
73. R. F. Newton
74. L. G. Overholser
75. J. D. Redman
76. J. H. Shaffer
77. R. J. Sheil
78. N. V. Smith
79. R. A. Strehlow
80. B. J. Sturm
81. W. T. Ward
82–91. R. E. Thoma
92. G. M. Watson
93. M. A. Bredig
94. S. Datz
95. R. E. Minturn
96. A. S. Dworkin
97. G. P. Smith
98. M. T. Robinson
99. A. J. Miller
100. L. G. Alexander
101. R. R. Dickison
102. G. W. Keilholtz
103. W. D. Manly
104. A. P. Fraas
105. L. A. Mann
106. F. R. Bruce
107. E. S. Bettis
108. R. P. Milford
109. R. A. Charpie
110. W. K. Ergen
111. R. B. Lindauer
112. J. C. White
113. A. S. Meyer
114. W. F. Vaughan
115. D. E. Ferguson
116. R. E. Blanco
117. J. T. Long
118. G. I. Cathers
119. W. H. Carr, Jr.
120. H. E. Goeller
121. H. F. McDuffie
122. W. L. Marshall

123. J. S. Gill
124. L. O. Gilpatrick
125. C. F. Baes
126. B. A. Soldano
127. W. E. Browning
128. M. J. Kelly
129. J. O. Blomeke
130. G. C. Williams
131. P. M. Reyling
132. J. Ricci (consultant)
133. C. E. Larson (consultant)
134. P. H. Emmett (consultant)
135. H. Eyring (consultant)
136. G. T. Seaborg (consultant)
137. ORNL – Y-12 Technical Library
Document Reference Section

EXTERNAL DISTRIBUTION

138. Division of Research and Development, AEC, ORO
139. Oak Ridge Institute of Nuclear Studies
140–142. University of Cincinnati (1 copy each to H. S. Green, J. W. Sausville, and T. B. Cameron)

138. Division of Research and Development, AEC, ORO
139. Oak Ridge Institute of Nuclear Studies
140–142. University of Cincinnati (1 copy each to H. S. Green, J. W. Sausville, and T. B. Cameron)
143. E. F. Osborn, Pennsylvania State University
144. G. W. Morey, 5806 Bradley Blvd., Bethesda, Md.
145–631. Distribution as shown in TID-4500 (14th ed.) under Chemistry-General category